

1 **Egg-derived anti-SARS-CoV-2 immunoglobulin Y (IgY)**  
2 **with broad variant activity as intranasal prophylaxis against**  
3 **COVID-19: preclinical studies and randomized controlled**  
4 **phase 1 clinical trial**

5  
6 **Short Title:** Intranasal egg-derived anti-SARS-CoV-2 IgY antibodies for passive immunization

7 **Authors:** Lyn R. Frumkin<sup>1¶</sup>, Michaela Lucas<sup>2¶</sup>, Curtis L. Scribner<sup>3</sup>, Nastassja Ortega-Heinly<sup>4</sup>,  
8 Jayden Rogers<sup>5</sup>, Gang Yin<sup>6</sup>, Trevor J Hallam<sup>6</sup>, Alice Yam<sup>6</sup>, Kristin Bedard<sup>6</sup>, Rebecca Begley<sup>1</sup>,  
9 Courtney A. Cohen<sup>7,8</sup>, Catherine V. Badger<sup>7</sup>, Shawn A. Abbasi<sup>7</sup>, John M. Dye<sup>7</sup>, Brian  
10 McMillan<sup>9</sup>, Michael Wallach<sup>10</sup>, Traci L. Bricker<sup>11</sup>, Astha Joshi<sup>11</sup>, Adrianus C.M. Boon<sup>11</sup>, Suman  
11 Pokhrel<sup>12</sup>, Benjamin R. Kraemer<sup>12</sup>, Lucia Lee<sup>12</sup>, Stephen Kargotich<sup>13</sup>, Mahima Agogiya<sup>1</sup>, Tom St.  
12 John<sup>14</sup>, Daria Mochly-Rosen<sup>1,12,13\*</sup>

13  
14 **Affiliations:**

15 <sup>1</sup> SPARK at Stanford, Stanford University, School of Medicine, Stanford, California, United  
16 States of America

17 <sup>2</sup> Faculty of Health and Medical Sciences Internal Medicine, The University of Western  
18 Australia, Perth, Western Australia, Australia

19 <sup>3</sup> Independent Regulatory Consultant, Oakland, California, United States of America

20 <sup>4</sup> Avian Vaccine Services, Charles River Laboratories, Storrs, Connecticut, United States of  
21 America

22 <sup>5</sup> Linear Clinical Research Ltd, Nedlands, Western Australia, Australia

23 <sup>6</sup> Sutro Biopharma Inc., South San Francisco, California, United States of America

24 <sup>7</sup> United States Army Medical Research Institute of Infectious Diseases, Virology Division,  
25 Frederick, Maryland, United States of America

26 <sup>8</sup> The Geneva Foundation, Tacoma, Washington, United States of America

27 <sup>9</sup> Bravado Pharmaceuticals, Lutz, Florida, United States of America

28 <sup>10</sup> University of Technology Sydney, Sydney, New South Wales, Australia and SPARK Sydney,  
29 Sydney, New South Wales, Australia

30 <sup>11</sup> Department of Medicine, Washington University School of Medicine, St. Louis, Missouri,  
31 United States of America

32 <sup>12</sup> Department of Chemical and Systems Biology, Stanford University, School of Medicine,  
33 Stanford, California, United States of America

34 <sup>13</sup> SPARK Global, Stanford University, School of Medicine, Stanford, California, United States  
35 of America

36 <sup>14</sup> Independent Scientist, Woodway, Washington, United States of America

37

38 ¶ These authors contributed equally to this work.

39 \*Corresponding author. Email: [mochly@stanford.edu](mailto:mochly@stanford.edu) (D.M-R)

40

41

## 42 **Abstract**

43 COVID-19 emergency use authorizations and approvals for vaccines were achieved in record  
44 time. However, there remains a need to develop additional safe, effective, easy-to-produce, and  
45 inexpensive prevention to reduce the risk of acquiring SARS-CoV-2 infection. This need is due  
46 to difficulties in vaccine manufacturing and distribution, vaccine hesitancy, and, critically, the  
47 increased prevalence of SARS-CoV-2 variants with greater contagiousness or reduced sensitivity  
48 to immunity. Antibodies from eggs of hens (immunoglobulin Y; IgY) that were administered  
49 receptor-binding domain (RBD) of the SARS-CoV-2 spike protein were developed as nasal  
50 drops to capture the virus on the nasal mucosa. Although initially raised against the 2019 novel  
51 coronavirus index strain (2019-nCoV), these anti-SARS-CoV-2 RBD IgY surprisingly had  
52 indistinguishable enzyme-linked immunosorbent assay binding against variants of concern that  
53 have emerged, including Alpha (B.1.1.7), Beta (B.1.351), Delta (B.1.617.2), and Omicron  
54 (B.1.1.529). This is distinct for sera from immunized or convalescent patients. Culture  
55 neutralization titers against available Alpha, Beta, and Delta were also indistinguishable from the  
56 index SARS-CoV-2 strain. Efforts to develop these IgY for clinical use demonstrated that the  
57 intranasal anti-SARS-CoV-2 RBD IgY preparation showed no binding (cross-reactivity) to a  
58 variety of human tissues and had an excellent safety profile in rats following 28-day intranasal  
59 delivery of the formulated IgY. A double-blind, randomized, placebo-controlled phase 1 study  
60 evaluating single-ascending and multiple doses of anti-SARS-CoV-2 RBD IgY administered  
61 intranasally for 14 days in 48 healthy participants also demonstrated an excellent safety and  
62 tolerability profile, and no evidence of systemic absorption. As these antiviral IgY have broad  
63 selectivity against many variants of concern, are fast to produce, and are a low-cost product, their  
64 use as prophylaxis to reduce SARS-CoV-2 viral transmission warrants further evaluation.

## 65 **Introduction**

66 As of January 4, 2022, over 290 million persons with coronavirus disease 2019 (COVID-19)  
67 had been identified in 222 countries and territories with an estimated 5.4 million deaths [1]. It  
68 is estimated that only 48% of the world population has been fully vaccinated [2], a figure  
69 dramatically lower than the 70%-80% believed needed to reach herd immunity to stop the  
70 pandemic [3,4]. Furthermore, only 8.5% of people in low-income countries have received at  
71 least one vaccine dose to date [2].

72 The fast emergency regulatory authorizations and approvals of COVID-19 vaccines in  
73 various countries were a critical turning point in slowing the spread of the pandemic. However,  
74 there remains a global need to develop additional safe, effective, easy-to-produce, and  
75 inexpensive prophylaxis to prevent or reduce the risk of acquiring severe acute respiratory  
76 syndrome coronavirus 2 (SARS-CoV-2) infection [5,6]. This need is due in part to the global  
77 shortage of essential components necessary for manufacturing the intramuscular mRNA  
78 vaccines and the requirement for cold chain storage for distribution. In addition, novel means  
79 of prevention are of heightened importance as variants of SARS-CoV-2 such as Delta  
80 (B.1.617.20) and Omicron (B.1.1.529) increase contagiousness and evade immunity produced  
81 by existing vaccines and previous infection [7-12] and where COVID-19 vaccination is  
82 unavailable, especially in resource-poor settings. The emergence of these variants has occurred  
83 even in populations with high vaccine uptake and are now the most prevalent COVID-19  
84 strains globally [13].

85 The main entry route for SARS-CoV-2 is the nasal mucosa, which has high levels of the  
86 human angiotensin-converting enzyme 2 (hACE2) receptor that is used by the virus to gain  
87 cellular entry [14]. Viral binding to the hACE2 receptor is mediated by the spike (S) protein on

88 the surface of the viral envelope [15] for all SARS-CoV-2 variants identified so far; even the  
89 highly mutated Omicron variant, with 15 mutations in the receptor-binding domain (RBD) of  
90 the S protein, is still dependent on hACE2 for its infectivity [16]. Therefore, the nasal mucosa  
91 is an excellent site as a critical barrier to reduce SARS-CoV-2 entry; antibodies against the  
92 SARS-CoV-2 RBD can compete with viral binding to the hACE2 receptor. In addition,  
93 antibodies on epithelial surfaces can greatly inhibit lateral viral motility, agglutinate viral  
94 particles, and anchor the virus to the extracellular matrix [17,18], thus making intranasally  
95 administered antibodies a potentially important antiviral strategy. Indeed, intranasal antibody  
96 prophylaxis has been an effective means against multiple viral pathogens in humans and  
97 veterinary applications, including respiratory tract viruses [18]. Thus, covering the nasal  
98 mucosa with anti-SARS-CoV-2 antibodies could prevent SARS-CoV-2 infection in naïve  
99 individuals and may also reduce viral transmission from an infected individual by reducing  
100 levels of active virus.

101 Because the RBD remains essential for SARS-CoV-2 infection, even for variants of  
102 concern, we chose recombinant RBD of the S protein (amino acids 328-533) as the  
103 immunogen. We next considered the optimal species to raise anti-SARS-CoV-2 polyclonal  
104 antibodies and chose to immunize egg-laying hens to enable fast, low-cost, and high-volume  
105 production. Antibodies generated in commercial hens (immunoglobulin Y; IgY) are  
106 concentrated in their eggs within 2-3 weeks following vaccination to 50-100 mg/egg, thus  
107 yielding up to 35 g of IgY per year; this yield can be up to five times higher (175 g of IgY in  
108 one year) when using specific pathogen-free (SPF) hens.

109 Here, we describe the production of anti-SARS-CoV-2 RBD IgY of the S protein in SPF  
110 hens and the characterization of these IgY, including in culture neutralization efficacy against

111 current pathogenic viral variants and a phase 1 study that evaluated the safety, tolerability, and  
112 pharmacokinetics of anti-SARS-CoV-2 RBD IgY given by intranasal drops in healthy humans.

## 113 **Materials and Methods**

### 114 **Study design**

115 The experiments were conducted in 4 parts: 1) production of immunogen (recombinant RBD),  
116 immunization of 12 SPF hens, IgY collection from egg yolks, and in vitro characterization of the  
117 IgY anti-SARS CoV-2 RBD, 2) GLP blinded safety studies in rat, treated intranasally twice daily  
118 for 28 days with a total of 16 mg/kg IgY or vehicle, 3) a preliminary efficacy study of hamsters  
119 treated with IgY or phosphate-buffered saline (PBS) for 4 hours before viral challenge, and 4) a  
120 placebo-controlled, double-blind phase 1 safety, tolerability, and pharmacokinetic (PK) study  
121 conducted in healthy humans using intranasal IgY or vehicle in single-ascending doses followed  
122 by multiple doses (3-times daily every 4 hours) for 14 days. Both the single-ascending and  
123 multiple-dose parts were followed by a 7-day nontreatment period to further evaluate safety.

### 124 **Recombinant SARS-CoV-2 RBD**

125 SARS-CoV-2 RBD (residues 328-533) of the 2019 novel coronavirus index virus (2019-  
126 nCoV) was expressed in cell-free protein synthesis reactions at Sutro Biopharma, Inc. (South San  
127 Francisco, CA) using the XpressCF™ platform [19,20] and was constructed as a carboxy-  
128 terminal fusion to a small ubiquitin-related modifier (SUMO) sequence to enable the production  
129 of a tagless RBD protein post enzymatic cleavage. The his-SUMO tag was constructed as  
130 previously described with an N-terminal his6-tag followed by a GGS-linker and the yeast SUMO  
131 protein Smt3 for Ulp1-enabled cleavage [19,20].

132 Briefly, cell-free reactions were prepared by the addition of 37.5% v/v iodoacetamide-  
133 treated S30 extract, 5 µg/mL plasmid, and a supermix containing amino acids, nano-  
134 microspheres, and small molecules for energy generation [20]. T7 RNA polymerase was over-  
135 expressed in *Escherichia coli* and added to the cell-free reaction as a reagent lysate at <1% v/v.  
136 Reactions were carried out in a DASbox stirred tank (Eppendorf) at 250 mL volume with pH,  
137 dissolved oxygen, and temperature control. Reactions were run for 16 hours at a temperature of  
138 25°C, pH was controlled at 7.0 using 1 M citrate and 1 M potassium hydroxide, and dissolved  
139 oxygen was maintained at 20%.

140 The XpressCF reaction of SARS-CoV-2-RBD 328-533 was clarified by centrifugation at  
141 10,000 rpm for 20 minutes (Beckman, JLA-10.500 rotor) and filtered through a 0.22-µm  
142 membrane filter. The clarified material was loaded onto a 5-mL his-Trap Excel affinity column  
143 equilibrated with binding buffer (15 mM Tris-HCl, 500 mM NaCl, pH 8.0). After 20 column  
144 volumes were applied to wash unbound impurities, the bound proteins were eluted with 20 mM  
145 Tris-HCl, 300 mM imidazole, pH 8.0. The eluted fractions were then analyzed by 4-12% sodium  
146 dodecyl sulfate-polyacrylamide gel electrophoresis (SDS-PAGE) and protein concentrations  
147 were determined by measured absorbance at 280 nm by NanoDrop (Thermo Fisher Scientific).  
148 The his-SUMO tag was removed by Ulp1 protease digestion for 1 hour at room temperature. The  
149 digested reaction was analyzed by 4-12% SDS-PAGE to verify full cleavage of the his-SUMO  
150 tag before flow-through mode purification by Capto Q (Cytiva). Twenty mM Tris-HCl, pH 8.0,  
151 was used to equilibrate the column, and the flow-through containing the cleaved protein was  
152 collected. To further purify the CoV-2-RBD, the Capto Q flow-through fraction was bound to a  
153 Capto SP ImpRes cation column equilibrated with 20 mM Tris-HCl, pH 8.0. The bound protein  
154 was eluted with a 30-column volume linear gradient using elution buffer (20 mM Tris-HCl, 300

155 mM NaCl, pH 8.0). An Amicon Ultra-15, 3kD centrifugal filter was used to concentrate and  
156 buffer exchange the target peak fraction into 6% sucrose in PBS at pH 7.2. The final purity of the  
157 product was demonstrated by high-performance liquid chromatography (HPLC) analysis.

## 158 **Characterization of the cell-free expressed recombinant RBD using surface** 159 **plasmon resonance**

160 Binding kinetic of cell-free expressed SARS-CoV-2 RBD construct or mammalian expressed  
161 his-tagged RBD control (ACROBiosystems SPD-C52H1) were then measured on a Biacore  
162 T200 instrument, using Fc-tagged hACE2 receptor protein (ACROBiosystems AC2-H5257). To  
163 this end, an anti-human Fc antibody (Jackson ImmunoResearch Labs) was immobilized on all  
164 flow cells of a CM5 chip (GE Healthcare). Fc-tagged human ACE2 receptor protein  
165 (ACROBiosystems AC2-H5257) was captured at ~100 replication units (RU). Binding of cell-  
166 free expressed SARS-CoV-2 S protein RBD construct or mammalian expressed RBD control  
167 (ACROBiosystems SPD-C52H1) was measured at concentrations up to 100 nM. Kinetic  
168 experiments were performed at 25°C at a flow rate of 50  $\mu$ L/min. RBD samples were diluted in  
169 HBS-EP buffer (Teknova) and injected over the chip for 180 seconds followed by a 420-second  
170 dissociation. The chip was regenerated with 10 mM glycine pH 1.5 after each injection.  
171 Affinities were calculated using Biacore T200 Evaluation Software.

## 172 **Hen immunization and IgY purification and characterization**

173 Nine SPF hens were obtained from Charles River Laboratories and housed in a filtered air,  
174 positive pressure barrier room (3 more hens from the same lot were added to the study after 5  
175 months) at Avian Vaccine Services, Charles River Laboratories (Storrs, CT). Each hen was  
176 caged individually with access to feed and water. Upon receipt, hens were immunized with an



177 inoculum containing 50 µg of recombinant cell-free expressed RBD fragment derived from S1  
178 spike protein and water-in-oil adjuvant. Test bleeds were taken before the first immunization and  
179 every 2 weeks after the first immunization throughout the project. Serum samples from each hen  
180 were tested using an indirect enzyme-linked immunoassay (ELISA) and Western blot. Hens  
181 received a boost 14 days after immunization and every 4 weeks after the previous immunization,  
182 unless otherwise indicated.

183 Eggs were collected weekly. Yolks in batches up to 100 eggs/batch were separated and  
184 IgY was purified. ELISA titration of IgY binding to full-length S1 (ACROBiosystems, S1N-  
185 C5255) expressed in human 293 cells and the cell-free expressed RBD of the SARS-CoV-2 spike  
186 protein was performed in 96-well plates. IgY was then purified from yolks. Eggs were collected  
187 weekly and egg white was separated from the egg yolk and discarded. Yolks were stored frozen  
188 at -20°C. For purification of IgY, yolks were thawed and diluted 1:10 in sterile PBS. The pH was  
189 reduced to 5.0 and the yolk solution was incubated at 4°C overnight. Yolk solution was then  
190 centrifuged for 10 minutes at 9000 rpm. Supernatant was removed, pooled, pH was increased to  
191 7.0, and final filtration (0.45 µm) was performed.

192 Hen sera and purified IgY were tested by ELISA and Western blot analysis using both  
193 the immunogen (RBD) and full length glycosylated S1 protein (ACROBiosystems, cat# S1N-  
194 C5255). Lot Y0120 of purified IgY was derived from 50 yolks, starting 2 weeks after the  
195 primary immunization. Lot Y0130 was derived from the next 50 yolks, starting 3 weeks after the  
196 primary immunization. Lot Y0140 and above were derived from the next 100 yolks collected  
197 over the preceding 2 weeks. Lots of purified IgY were tested by indirect ELISA and Western  
198 blot to determine antibody response levels within the yolk after purification as well as affinity to  
199 the cell-free expressed RBD fragment of S1 spike protein and the entire glycosylated S1 protein

200 (ACROBiosystems, cat# S1N-C5255). Protein concentration was also measured using the  
201 Bradford assay. IgY purity was determined using SDS-PAGE under reducing conditions and  
202 stained with Coomassie Blue.

203 ELISA titration of IgY binding to full length and the RBD of the SARS-CoV-2 spike  
204 protein was performed as follows: 96-well clear flat bottom polystyrene high-binding ELISA  
205 plates (Corning, Cat# 9018) were coated with 100  $\mu$ l/well of 5  $\mu$ g/mL recombinant his-tagged  
206 (Sino Biological) RBD protein overnight at 4°C. Plates were then washed twice with PBS and  
207 blocked with 1% bovine serum albumin (BSA)-PBS. After blocking, 100  $\mu$ L of serial dilutions  
208 of IgY were added to the wells and incubated at room temperature for 2 hours. The plates were  
209 then washed twice and incubated with horseradish peroxidase (HRP)-conjugated mouse rat anti-  
210 chicken IgY (Sapphire, Cat# LO-IgY-16-P-0.5 ) 1:2000 diluted in 0.5% BSA and 0.05% Tween-  
211 20 in PBS) for 60 minutes. After 3 final washes using 0.05% PBS-Tween, the plates were read  
212 using chemiluminescent substrate (Pierce TMB Substrate Kit, Thermo Fisher, Cat# 34021).  
213 Luminescence was read on a plate reader and analyzed with SoftMaxPro 6.0 (Molecular  
214 Devices).

215 Hen sera were diluted with 1% BSA at various dilutions and tested in ELISA. One  
216 hundred microliters were added to wells and the plate was incubated at room temperature for 1  
217 hour. Plate wells were then rinsed with 1% Tween 20 wash solution, as indicated above. Anti-  
218 chicken HRP conjugate (Invitrogen, cat# SA-19509) diluted 1:5000 was added to each well. The  
219 plate was incubated at room temperature for 1 hour, followed by another 1% Tween 20 wash.  
220 3,3',5,5'-tetramethylbenzidine substrate (KPL, cat# 5120-0050) was added to each well and the  
221 plate was incubated at room temperature for 15 minutes. Optical density was measured using an  
222 ELISA reader (Molecular Devices) at 650 nm.

223 Western blot analysis was performed with the cell-free expressed RBD fragment of the  
224 index S1 protein or the entire mammalian-expressed S1 protein (ACROBiosystems). One  
225 microgram of denatured protein was added to Mini-PROTEAN TGX 4-20% SDS-PAGE. Gel  
226 was run at 200V for 45 minutes in Tris-glycine buffer and stained using Simply Blue Safestain  
227 (Invitrogen) at room temperature for 1 hour. Gels were destained twice using deionized water.

228 An unstained SDS-PAGE gel was transferred to the polyvinylidene difluoride membrane  
229 using Trans-Blot Turbo Transfer System (Bio-Rad Laboratories) and cut into strips. Strips were  
230 then stored at -20°C until ready to use. Five percent nonfat dry milk was added to strips and  
231 incubated at room temperature for 30-60 minutes. Test bleed sera and IgY were diluted 1:2000  
232 and purified IgY were diluted 1:500 in 0.2 µm-filtered PBS and added to strips. Strips were  
233 incubated at room temperature for 2 hours followed by 3 washes in filtered PBS. Rabbit anti-  
234 chicken IgY (H+L) secondary antibody, HRP (Invitrogen) diluted 1:3000 was added to each strip  
235 and incubated at room temperature for 1-2 hours. Strips were washed once again in filtered PBS.  
236 Opti-4CN substrate (Bio-Rad Laboratories) was added to each strip and incubated at room  
237 temperature for up to 30 minutes in a rocking incubator. Strips were washed twice in deionized  
238 water and images were taken using Bio-Rad EZ Gel Imager.

### 239 **ELISA evaluation of IgY titer against SARS-CoV-2 variants of concern**

240 ELISA titer of the final IgY preparation used in the clinical studies against the Alpha, Beta,  
241 Delta, and Omicron-derived RBD [amino acids 319-537; ACROBiosystems SPD-C52H1(index),  
242 SPD-C52Hn (Alpha), SPD-C52Hp (Beta), SPD-C525e (Delta), and SPD-C522e (Omicron)] was  
243 carried out as described above.

### 244 **In culture viral neutralization studies using pseudovirus**

245           The neutralization assays using pseudovirus were performed at RetroVirox (San Diego,  
246 CA). The assay used 3 non-replicative vesicular stomatitis virus (VSV) pseudoviruses carrying a  
247 firefly luciferase reporter gene and expressing the following S protein of SARS-CoV-2 on the  
248 surface: the index SARS-CoV-2 Hu-1 spike, a truncated spike with a C-terminal 19 amino acid  
249 deletion; the Beta variant (K417N/ E484K / N501Y / D614G full-length spike); and a D614G  
250 spike variant with a full-length sequence of the index spike protein. The IgY preparation or  
251 plasma was diluted in Dulbecco's Modified Eagle Medium (DMEM) with 5% fetal bovine serum  
252 (FBS) to perform pre-incubation with pseudovirus before addition to target cells. The  
253 neutralization assay was performed with HEK 293T-hACE2, a human embryonic kidney cell  
254 line overexpressing hACE2. Test item was preincubated for 60 minutes at 37°C with a  
255 previously titrated inoculum of pseudovirus. The mixture was then added to 293T-hACE2 cells  
256 and infection was allowed for 24 hours. Pseudovirus infection was determined by measuring  
257 firefly luciferase activity (RLU, relative light unit ratio) 24 hours after infection. Putative  
258 neutralizing antibodies (human sera, purified IgY, or vehicle) were present in the cell culture for  
259 the entire duration of the experiment. The ability of the test item to neutralize pseudovirus  
260 carrying SARS-CoV-2 spike was compared with samples treated with vehicle alone. Nine  
261 concentrations of the IgY sample were tested in duplicates with each variant in 5-fold serial  
262 dilutions starting at 10,000 µg/mL. The half-maximal inhibitory concentration (IC<sub>50</sub>) and 50%  
263 neutralization titer (NT<sub>50</sub>) values for the IgY and positive control human serum were determined  
264 using GraphPad Prism software (GraphPad Software).

265           Quality controls for the pseudovirus neutralization assays were performed to determine:  
266 1) signal-to-background values; 2) variation of the assay, estimated as the average of the  
267 coefficient of variation for data points for which 50% or greater infection (RLUs) was observed

268 compared to cells with pseudovirus in the presence of vehicle alone, and 3) neutralization with  
269 plasma from an individual who received 2 doses of the Moderna (mRNA-1273) COVID-19  
270 vaccine. All controls worked as anticipated for each assay.

### 271 **In culture neutralization studies using live virus**

272 At United States Army Medical Research Institute of Infectious Diseases (USAMARIID;  
273 Frederick, MD), all work with authentic (live) SARS-CoV-2 was completed in Biosafety Level 3  
274 laboratories following federal and institutional biosafety standards and regulations. Vero-76 cells  
275 were inoculated with SARS-CoV-2/Was1 (MT020880.1) at a multiplicity of infection of 0.01  
276 and incubated at 37°C with 5% CO<sub>2</sub> and 80% humidity. At 50 hours post-infection, cells were  
277 frozen at -80°C for 1 hour, allowed to thaw at room temperature, and supernatants were collected  
278 and clarified by centrifugation at ~2,500 ×g for 10 minutes. Clarified supernatant was aliquoted  
279 and stored at -80°C.

280 Authentic (live) SARS-CoV-2/B.1.617.2 at a multiplicity of infection of 1 was incubated  
281 for 1 hour at 37°C with serially diluted antibodies. Vero-E6 monolayers were exposed to the  
282 antibody-virus mixture at 37°C for 1 hour. Following incubation, viral inoculum was removed  
283 and fresh cell culture media was added for an additional 23 hours at 37°C. Cells were washed  
284 with PBS, fixed in 10% formalin, and permeabilized with 0.2% Triton-X for 10 minutes.  
285 Detection of infection was accomplished using an anti-SARS-CoV-2 nucleocapsid protein  
286 detection antibody (Sino Biological), and a goat α-rabbit secondary antibody conjugated to  
287 AlexaFluor488. Infected cells were identified using the PerkinElmer Operetta high-content  
288 imaging instrument and data analysis was performed using the Harmony software (PerkinElmer).

289 At RetroVirox (San Diego, CA), purified IgY (lot Y0180) was tested against two live  
290 SARS-CoV-2 clinical isolates: MEX-BC15/2021 (lineage B.1.617.2, Delta variant) and MEX-

291 BC2/2020 (lineage B.1, carrying the D614G mutation). A virus-induced cytopathic effect (CPE)-  
292 based neutralization assay was performed by infecting Vero E6 cells in the presence or absence  
293 of test items. Vero E6 cells were maintained in DMEM with 10% FBS. Twenty-four hours after  
294 cell seeding, test samples were submitted to serial dilutions with DMEM with 2% FBS in a  
295 different plate. Then, virus diluted in the same media alone was pre-incubated with test items for  
296 1 hour at 37°C in a humidified incubator. Following incubation, media was removed from cells.  
297 Cells were then challenged with the SARS-CoV-2/antibody pre-incubated mix. The amount of  
298 viral inoculum was previously titrated to result in a linear response inhibited by antivirals with  
299 known activity against SARS-CoV-2. Cell culture media with the virus inoculum was not  
300 removed after virus adsorption, and antibodies and virus were maintained in the media for the  
301 duration of the assay (96 hours). After this period, the extent of cell viability was monitored with  
302 the neutral red uptake assay.

303 The virus-induced CPE was monitored under the microscope after 3 days of infection,  
304 and cells were stained with neutral red to monitor cell viability the following day. Viable cells  
305 incorporate neutral red in their lysosomes. The uptake of neutral red relies on the ability of live  
306 cells to maintain the pH inside the lysosomes lower than in the cytoplasm, a process that requires  
307 ATP. Inside the lysosome, the dye becomes charged and is retained. After a 3-hour incubation  
308 with neutral red (0.017%), the extra dye is washed away, and the neutral red is extracted from  
309 lysosomes by incubating cells for 15 minutes with a solution containing 50% ethanol and 1%  
310 acetic acid. The amount of neutral red is estimated by measuring absorbance at 540 nm in a plate  
311 reader.

312 Antibodies were evaluated in triplicates using five-fold serial dilutions starting at 10.0  
313 mg/mL. Controls included uninfected cells and infected cells treated with vehicle alone. Some

314 cells were treated with plasma from an uninfected individual who received two doses of  
315 Moderna's mRNA COVID-19 vaccine as a positive control.

### 316 **CPE-based neutralization assay**

317 The average absorbance at 540 nm (A540) observed in infected cells in the presence of vehicle  
318 alone was calculated, and then subtracted from all samples to determine the inhibition of the  
319 virus-induced CPE. Data points were then normalized to the average A540 signal observed in  
320 uninfected cells after subtraction of the absorbance signal observed in infected cells. In the  
321 neutral red CPE-based neutralization assay, uninfected cells remained viable and uptake the dye  
322 at higher levels than non-viable cells. In the absence of test items, the virus-induced CPE kills  
323 infected cells and leads to lower A540 (this value equals 0% inhibition). In contrast, incubation  
324 with neutralizing agents prevents the virus-induced CPE and leads to absorbance levels similar to  
325 those observed in uninfected cells. Full recovery of cell viability in infected cells represents  
326 100% neutralization of the virus.

### 327 **GMP IgY formulation, analytical studies, and stability**

328 Using Good Manufacturing Practice (GMP), anti-S1 RBD IgY was formulated for use as  
329 intranasal drops as 0 (placebo control), 5, 10, and 20 mg/mL anti-S1 RBD IgY preparations in  
330 sterile 2% microcrystalline cellulose and carboxymethylcellulose sodium at Bravado  
331 Pharmaceuticals (Lutz, FL). The suspension was packed in a 1.5-mL dropper bottle and tests for  
332 GMP drug product release complied with the relevant standards and methods, including  
333 microbiological examination of nonsterile products (USP <1111>, <61> and <62>). All  
334 formulated products were 100% stable as measured by physical and analytical properties,  
335 including HPLC, when stored for at least 6 months at 2-8°C and about 1 month when stored at  
336 room temperature. Ten and 20 mg/mL solutions stored at room temperature showed 100%

337 analytical stabilities for 3 months. However, several samples had some physical visual  
338 abnormalities (slight discoloration and opacity) that occurred beginning at 1 month when stored  
339 at room temperature. Therefore, all formulated samples used in the subsequent studies were  
340 stored at 2-8°C. For stability determination, formulated IgY (20 mL) was chromatographed on a  
341 TSK Gel G3000swxl sizing column (with guard column) on HPLC at 0.4 mL/min at room  
342 temperature, and eluate was monitored at 214 nm. For the rat toxicity and safety study, and for  
343 the human study, we used only 20 mg/mL as the highest dose because it was readily soluble.

### 344 **GLP rat toxicity and safety study**

345 Thirty-eight female and 38 male >8-week-old Sprague Dawley rats were used in a GLP study  
346 conducted at Charles River Laboratories (Spencerville, OH). Rats were identified using a  
347 subcutaneously implanted electronic identification chip and were acclimated to their housing for  
348 at least 4 days before the first day of dosing. Animals were randomly assigned to groups; males  
349 and females were randomized separately and housed in accordance with the USDA Animal  
350 Welfare Act (9 CFR, Parts 1, 2 and 3) and as described in the Guide for the Care and Use of  
351 Laboratory Animals.

352 For psychological and environmental enrichment, a hiding device, a chewing object, and  
353 edible enrichment treats were offered throughout the study and a cycle of 12 hours light and 12  
354 hours dark was maintained. Water and food were freely available. The experimental protocol is  
355 summarized in S1-S3 Tables.

356 Detailed clinical observation was conducted once a week and included body weight and  
357 food consumption. Ophthalmic examinations were conducted before treatment and during the  
358 last week of dosing by a veterinary ophthalmologist and included a short-acting mydriatic  
359 solution treatment to each eye to facilitate the ocular examinations. Clinical laboratory



360 assessments included hematology, coagulation, clinical chemistry, urinalysis, and presence of  
361 circulating IgY (in serum) tested on pretreatment and Day 28 (last day of treatment) after 4 hours  
362 of fasting.

363 Hematology parameters included red blood cell count, hemoglobin concentration,  
364 hematocrit, mean corpuscular volume, red blood cell distribution width, mean corpuscular  
365 hemoglobin concentration, mean corpuscular hemoglobin, reticulocyte count (absolute), platelet  
366 count, white blood cell count, neutrophil count (absolute), lymphocyte count (absolute),  
367 monocyte count (absolute), eosinophil count (absolute), basophil count (absolute), large  
368 unstained cells (absolute) and other cells (as appropriate). Clinical chemistry parameters included  
369 alanine aminotransferase, aspartate aminotransferase, alkaline phosphatase, gamma-  
370 glutamyltransferase, creatine kinase, total bilirubin, urea nitrogen, creatinine, calcium,  
371 phosphorus, total protein, albumin, globulin (calculated), albumin/globulin ratio, glucose,  
372 cholesterol, triglycerides, sodium, potassium, chloride, and sample quality. Urinalysis included  
373 color, appearance/clarity, specific gravity, volume, pH, protein, glucose, bilirubin, ketones, and  
374 blood.

### 375 **Cytokine level measurement and analysis**

376 This non-GLP blinded assay was performed on serum by the Immunoassay Team at the Human  
377 Immune Monitoring Center at Stanford University (Stanford, CA). Assay kits  
378 (RECYMAG65K27PMX Rat) were purchased from EMD Millipore and used according to the  
379 manufacturer's recommendations, with modifications described as follows. Briefly, samples  
380 were mixed with antibody-linked magnetic beads on a 96-well plate and incubated overnight at  
381 4°C while shaking. Cold and room temperature incubation steps were performed on an orbital  
382 shaker at 500-600 rpm. Plates were washed twice with wash buffer in a Biotek ELx405 washer.

383 Following 1-hour incubation at room temperature with a biotinylated detection antibody,  
384 streptavidin-PE was added for 30 minutes while shaking. Plates were washed as described above  
385 and PBS was added to wells for reading in the Luminex FLEXMAP 3D Instrument with a lower  
386 bound of 50 beads per sample per cytokine. Each sample was measured in duplicate. Custom  
387 Assay Chex control beads were purchased from Radix BioSolutions and added to all wells.

388 Median fluorescence intensity (MFI) data were corrected for plate and nonspecific  
389 binding artifacts [20]. Corrected MFI was regressed on time point. Regression analysis employed  
390 linear mixed models [21] in SAS®/STAT (SAS Institute) with a separate model fit for each  
391 treatment and cytokine, and with separate sets of models with and without gender as a covariate,  
392 for 108 models in total. Of the 108 models, 84% met the assumption of normally distributed  
393 residuals and 78% for random effects.

#### 394 **IgY in sera of treated rats**

395 The presence of anti-SARS-CoV-2 IgY in sera of rats was evaluated using GLP standards in a  
396 qualified ELISA assay at Charles River Laboratories (Reno, NV). ELISA 96-well plates were  
397 coated with goat anti-chicken IgY (Thermo Fisher; A16056). After blocking, the plates were  
398 incubated with the samples containing anti-SARS-CoV-2 IgY at various concentrations for 1  
399 hour at room temperature. After washing the microplate, rabbit anti-chicken IgY (Thermo Fisher;  
400 A16130) - HRP conjugate was added and incubated for 1 hour at room temperature. The ELISA  
401 plate was washed and substrate (3,3',5,5'-tetramethylbenzidine) was added to the wells and  
402 incubated for 20 minutes. The color development was stopped by the addition of 2N sulfuric acid  
403 and color intensity measured in a microplate reader at 450 nm. A calibration curve from the  
404 absorbance values was obtained from the standards using a 4-parameter curve fit with a

405 weighting equation of  $1/y^2$ . The concentrations of anti-SARS-CoV-2 IgY in the samples were  
406 determined from the calibration curve. After 4 analytical method validations, lower and upper  
407 limit of detection, intra- and inter-assay precision and accuracy, dilution integrity, and short-term  
408 stability, IgY levels in the blood samples of rats before and after 28 days of treatment were  
409 below the limit of detection.

## 410 **Human tissue cross-reactivity study**

411 A GLP study examining human tissue reactivity of the anti-SARS-CoV-2 RBD IgY was  
412 conducted at Charles River Laboratories (Frederick, MD) using at least 3 tissues from at least 3  
413 donors (S4 Table). Ten mL of 10 mg/mL or 20 mg/mL IgY control (negative control) and anti-  
414 SARS-CoV-2 RBD IgY or an anti-human hypercalcemia of malignancy peptide (amino acid  
415 residues 1-34, Sigma-Aldrich; Catalog No. H9148; positive control), each in 1% BSA, were  
416 incubated for 1 hour with acetone-fixed human tissues (normal) of at least 3 separate donors after  
417 20 minutes incubation with block solution of PBS + 1% BSA, 0.5% casein and 5% normal rabbit  
418 serum. After PBS washes, the secondary antibody (peroxidase [HRP]-conjugated rabbit anti-  
419 chicken IgY; Testing Facility antibody tracking No. A45764; of 2  $\mu\text{g}/\text{mL}$ ) was added for 30  
420 minutes. After PBS washes, DAB (3,3'-diaminobenzidine) was applied for 4 minutes as a  
421 substrate for the peroxidase reaction. All slides were rinsed with tap water, counterstained,  
422 dehydrated, and mounted for visualization. For the  $\beta$ 2-microglobulin antibody (positive control  
423 staining) 1  $\mu\text{g}/\text{mL}$  of antibodies were incubated with the slides for 1 hour and bound antibodies  
424 were detected with biotinylated secondary antibody (goat anti-rabbit IgG; 2  $\mu\text{g}/\text{mL}$ ) for 30  
425 minutes, as above. The slides were then visualized on light microscopy.

## 426 **Virus preparation for the efficacy study in a hamster model of** 427 **COVID-19 and quantitation of viral load in the animals**

428 Syrian hamsters develop mild-to-moderate disease with progressive weight loss that starts  
429 several days after SARS-CoV-2 infection by intranasal inoculation [22,23]. SARS-CoV-2 (strain  
430 2019-nCoV/USA-WA1/2020) was propagated on Vero-TMPRSS2 cells, and the virus titer was  
431 determined by plaque assays on Vero-hACE2 and Vero-hACE2-TMPRSS2 cells. Briefly, cells  
432 were seeded in 24-well plates, and the next day, virus stocks were serially diluted 10-fold,  
433 starting at 1:10, in cell infection medium [Minimum Essential Media (MEM) containing 2%  
434 FBS, L-glutamine, penicillin, and streptomycin]. Two hundred and fifty microliters of the diluted  
435 virus were added to a single well per dilution per sample. After 1 hour at 37°C, the inoculum was  
436 aspirated and a 1% methylcellulose overlay in MEM supplemented with 2% FBS was added.  
437 Seventy-two hours after virus inoculation, the cells were fixed with 4% formalin and the  
438 monolayer was stained with crystal violet (0.5% w/v in 25% methanol in water) for 1 hour at  
439 20°C. The number of plaques was counted and used to calculate the plaque-forming units  
440 (PFU)/mL.

#### 441 **Study protocol: hamster infection with SARS-CoV-2**

442 Five- to 6-week-old Syrian golden hamsters (Charles River Laboratories) infected with SARS-  
443 CoV-2 as previously described [23] were housed at the Washington University (St. Louis, MO)  
444 Biosafety Level 3 facility in HEPA-filtered rodent cages. Before challenge with SARS-CoV-2,  
445 all animals received 100 µL of a placebo control fluid or fluid-formulated anti-SARS-CoV-2  
446 RBD IgY (1 mg/50 mL of the 20 mg/mL solution per nare). The amount of nasal anti-SARS-  
447 CoV-2 RBD IgY drops was limited by the volume that could be given per nare. Four hours after  
448 the delivery, animals were challenged with  $10^4$  or  $5 \times 10^4$  PFU of SARS-CoV-2 (titer determined  
449 on Vero-hACE2; see below). The protocol included 18 hamsters in 4 planned groups: Group 1:  
450 Control with high  $5 \times 10^4$  PFU (4 animals); Group 2: Control with  $1 \times 10^4$  PFU (4 animals);  
451 Group 3: Anti-SARS-CoV-2 RBD IgY with  $5 \times 10^4$  PFU (5 animals); and Group 4: Anti-SARS-

452 CoV-2 RBD IgY with  $1 \times 10^4$  PFU (5 animals). Note that the viral titer in Vero-hACE2-  
453 hTMPRSS2 cells, which express the essential protease to liberate the RBD from the S protein on  
454 the surface of the virus [24], was subsequently found to be almost 100-fold higher for Groups 1  
455 and 3 ( $4 \times 10^6$  PFU) and Groups 2 and 4 ( $0.8 \times 10^6$  PFU).

456 Animal weight was recorded daily. Three days after challenge, the animals were  
457 sacrificed and lungs were collected. The left lobe was homogenized in 1.0 mL of DMEM and the  
458 clarified supernatant was used for viral load analysis by plaque assay and quantitative reverse  
459 transcription PCR (RT-qPCR).

#### 460 **Virus titration assays from hamster samples**

461 Plaque assays were performed on Vero-hACE2 and Vero-hACE2-TMPRSS2 cells in 24-well  
462 plates. Lung tissue homogenates were serially diluted 10-fold, starting at 1:10, in cell infection  
463 medium (DMEM containing 2% FBS, L-glutamine, penicillin, and streptomycin). Two hundred  
464 and fifty microliters of the diluted lung homogenates were added to a single well per dilution per  
465 sample. After 1 hour at 37°C, the inoculum was aspirated and a 1% methylcellulose overlay in  
466 MEM supplemented with 2% FBS was added. Seventy-two hours after virus inoculation, the  
467 cells were fixed with 4% formalin, and the monolayer was stained with crystal violet (0.5% w/v  
468 in 25% methanol in water) for 1 hour at 20°C. The number of plaques was counted and used to  
469 calculate the PFU/mL. To quantify viral load in lung tissue homogenates, RNA was extracted  
470 from 100  $\mu$ L samples using QIAamp viral RNA mini kit (Qiagen) and eluted with 50  $\mu$ L of  
471 water. RNA (4  $\mu$ L) was used for real-time RT-qPCR to detect and quantify N gene of SARS-  
472 CoV-2 using TaqMan™ Fast Virus 1-Step Master Mix (Applied Biosystems) or using the  
473 following primers and probes for the N-gene, forward: GACCCCAAATCAGCGAAAT;  
474 reverse: TCTGGTTACTGCCAGTTGAATCTG, probe:

475 ACCCCGCATTACGTTTGGTGGACC, or the 5'-UTR, forward:  
476 ACTGTCGTTGACAGGACACG, reverse: AACACGGACGAAACCGTAAG, probe:  
477 CGTCTATCTTCTGCAGGCTG. Viral RNA was expressed as gene copy numbers per mg for  
478 lung tissue homogenates and per mL for nasal swabs, based on a standard included in the assay  
479 that was created by in vitro transcription of a synthetic DNA molecule containing the target  
480 region of the N gene or 5'-UTR.

## 481 **Statistical Analysis**

482 Data were analyzed with GraphPad Prism 9.0 and statistical significance was assigned when P  
483 values were < 0.05. All tests and values are indicated in figure legends.

## 484 **Phase 1 safety, tolerability, and pharmacokinetic study in humans**

### 485 **Study design and dose selection**

486 A single-center, randomized, double-blind, placebo-controlled phase 1 study of anti-SARS-CoV-  
487 2 RBD IgY given intranasally to 48 healthy adults was conducted at Linear Clinical Research-  
488 Harry Perkins Research Institute (Perth, WA, Australia) (Fig. 1, S1 CONSORT Checklist).  
489 Written informed consent was obtained from all participants. The study is registered at  
490 ClinicalTrials.gov: NCT04567810. The study period was conducted between September 25,  
491 2020 and December 14, 2020. The protocol for this trial and the supporting CONSORT checklist  
492 are available as supporting information (S1 Protocol and S1 CONSORT checklist).

### 493 **Figure 1.** CONSORT flow diagram of phase 1 single-ascending and multiple-dose study

494 The primary objective of the study was to assess the safety and tolerability of anti-SARS-  
495 CoV-2 IgY. A secondary objective was to assess the PK of anti-SARS-CoV-2 IgY. Evaluation of  
496 immunoglobulin E (IgE) and anti-IgE antibodies was an exploratory objective.

497 Healthy male and female participants  $\geq 18$  and  $\leq 45$  years old with a body weight  $\geq 50$  kg  
498 and a body mass index  $\geq 18.0$  and  $\leq 32.0$  kg/m<sup>2</sup> were eligible for this study. Females of  
499 childbearing potential who were pregnant or lactating or planning to become pregnant during the  
500 study and participants with a history of alcohol and drug abuse, current smoking, clinically  
501 significant laboratory abnormalities, history of nasal surgical procedures, frequent or recurrent  
502 nasal conditions, current use of any nasal preparations, evidence of or history of clinically  
503 significant conditions, or positive test for hepatitis B, hepatitis C, human immunodeficiency  
504 virus, or SARS-CoV-2 nucleic acid or serology were excluded from participation. Full eligibility  
505 criteria are summarized in S1 Protocol.

506 The master randomization schedule and the associated code break envelope files were  
507 produced by an unblinded statistician using a computer-generated (SAS® v9.4 PLAN procedure)  
508 pseudo-random permutation procedure. For Part 1, the first two randomization numbers for each  
509 cohort were randomly assigned in a 1:1 ratio (anti-SARS-CoV-2 IgY: Placebo) to allow for  
510 sentinel dosing, and the remainder of the numbers for each cohort was generated in a 5:1 (anti-  
511 SARS-CoV-2 IgY: Placebo) ratio using a permuted blocked randomization with a block size of  
512 six. For Part 2, 24 numbers were generated in a 1:1:1:1 ratio (6 mg anti-SARS-CoV-2 IgY: 12  
513 mg anti-SARS-CoV-2 IgY: 24 mg anti-SARS-CoV-2 IgY: Placebo) using a permuted blocked  
514 randomization with a block size of six. The block sizes were kept confidential during the study.

515 The site personnel randomized eligible participants on Day 1 by assigning the next  
516 available randomization number for the specific study part to the participant and reporting the  
517 randomization number on the case report form. Study drug was prepared by an unblinded  
518 pharmacist based on the treatment corresponding to the assigned randomization number on the

519 randomization schedule that was only available to the pharmacist. In the event of an emergency,  
520 authorized personnel were able to unblind a participant through the code break envelope  
521 associated with the randomization number assigned to the participant.

522 In Part 1, participants were randomly assigned to receive a single dose of anti-SARS-  
523 CoV-2 RBD IgY antibodies or placebo in a sequential escalating manner. Three groups were  
524 sequentially dosed with 8 healthy participants per group (6 active and 2 placebo in each group).  
525 Each group in Part 1 included the initial dosing of a sentinel group (1 anti-SARS-CoV-2 RBD  
526 IgY and 1 placebo) at least 24 hours before dosing the remaining 6 participants in the cohort (5  
527 anti-SARS-CoV-2 RBD IgY and 1 placebo). The remainder of the cohort were dosed if, in the  
528 opinion of the investigator, there were no significant safety concerns identified in the sentinel  
529 participants within the first 24 hours after administration of the dose (anti-SARS-CoV-2 RBD  
530 IgY or placebo). A Safety Monitoring Committee (SMC) reviewed safety data before each dose  
531 escalation. The following regimens were administered: 2 mg anti-SARS-CoV-2 RBD IgY  
532 preparation or placebo, 4 mg anti-SARS-CoV-2 RBD IgY preparation or placebo, and 8 mg anti-  
533 SARS-CoV-2 RBD IgY preparation or placebo. In Part 1, 2 drops were applied to each nostril as  
534 a single administration. A 7-day nontreatment follow-up period assessed safety after completion  
535 of the dosing.

536 In Part 2, participants were randomly assigned to receive multiple daily administrations  
537 of anti-SARS-CoV-2 RBD IgY or placebo every 4 hours (3-times daily) for 14 days in a parallel-  
538 group manner. Up to 24 healthy participants were randomized to 1 of 4 treatment regimens (6  
539 participants per regimen). The following regimens were administered: 6 mg total daily dose anti-  
540 SARS-CoV-2 RBD IgY preparation for 14 days, 12 mg total daily dose anti-SARS-CoV-2 RBD  
541 IgY preparation for 14 days, 24 mg total daily dose anti-SARS-CoV-2 RBD IgY preparation for



542 14 days, and 0 mg total daily dose placebo preparation for 14 days. In Part 2, 2 drops were  
543 applied to each nostril every 4 hours (3-times daily). A 7-day nontreatment follow-up period  
544 assessed safety after completion of the dosing.

545 In each part, 3 groups with 8 healthy participants per group (6 active and 2 placebo in  
546 each group) were dosed. Safety and tolerability were evaluated using adverse event, physical  
547 examination (including vital signs), electrocardiogram, and clinical laboratory data. PK of anti-  
548 SARS-CoV-2 RBD IgY was evaluated by measuring serum concentrations pretreatment and at  
549 Day 14 when given as multiple doses administered intranasally for 14 days.

550 The investigational drug was supplied as a liquid preparation in a nose drop bottle  
551 containing 1.5 mL anti-SARS-CoV-2 RBD IgY preparation nasal suspension at 5, 10, or 20  
552 mg/mL, or placebo, for intranasal application. Each bottle of nasal drops had enough material for  
553 one day of use. The liquid preparation contained anti-SARS-CoV-2 RBD IgY 0.5 mg/100  
554  $\mu$ L/drop, 1 mg/100  $\mu$ L/drop, or 2 mg/100  $\mu$ L/drop. The total maximum daily dose of anti-SARS-  
555 CoV-2 RBD IgY used in the present study (24 mg) was based in part on solubility considerations  
556 and is less than the daily dose of anti- *Pseudomonas aeruginosa* IgY previously given  
557 prophylactically as an oral treatment to prevent pulmonary infections in 17 patients with cystic  
558 fibrosis [25]. For the maximum anti-SARS-CoV-2 RBD IgY dose of 4 mg/nare, we calculated a  
559 favorable ratio of IgY to viral particles, even when virus covers the nasal pathway.

560 All participants were provided with a Dose Administration Guide and instructed to  
561 “Gently blow your nose before using this drug. Then tilt your head back while sitting or lying  
562 down. After the study drug is administered, keep your head tilted for a few minutes. Try not to  
563 blow your nose for at least 5 minutes after study drug administration.”

## 564 **Assessments**

565 Safety (and tolerability) were evaluated using adverse event, physical examination (including  
566 vital signs), electrocardiogram, and clinical laboratory data that included nonfasted collection of  
567 a) hematology (hemoglobin, hematocrit, erythrocyte count, mean cell volume, neutrophils,  
568 lymphocytes, monocytes, eosinophils, basophils, platelets, reticulocyte count), b) serum  
569 metabolic panel (sodium, potassium, chloride, total bilirubin, alkaline phosphatase, alanine  
570 transaminase, aspartate transaminase, blood urea nitrogen, creatinine, uric acid, phosphorous,  
571 calcium, plasma glucose, total protein, albumin, cholesterol, creatinine kinase, c) coagulation, d)  
572 urinalysis, and e) urine human chorionic gonadotropin values. Pharmacokinetics following  
573 intranasal administration of anti-SARS-CoV-2 RBD IgY were evaluated in the multiple-dose  
574 part of the study by measuring serum anti-SARS-CoV-2 RBD IgY concentration (lower limit of  
575 quantification, 30 ng/mL) at baseline and 2 hours after final dosing on Day 14, as described  
576 above (Charles River Laboratories, Reno, NV).

577 Serum cytokine levels for exploratory analyses were evaluated from the sera of 19  
578 multiple-dose participants before and 2 hours after dosing on Days 1 and 2, as described above  
579 (Stanford Human Immune Monitoring Center, Stanford CA). An exploratory analysis was  
580 conducted of pretreatment serum total IgE and anti-IgE antibody (mainly anti-ovalbumin) levels  
581 in the 24 participants in the multiple-dose part of the trial.

## 582 **Changes in the Conduct of the Study**

583 All participants were enrolled, treated, and assessed under Protocol CVR001 version 3.0, dated  
584 29 September 2020 (S1 Protocol). The following changes were made to the conduct of the study  
585 from what was specified in the protocol:

- 586 • Participants were reconsented to allow for exploratory cytokine analyses on stored blood  
587 samples.
- 588 • Per the study protocol, serum anti-SARS-CoV-2 IgY samples were obtained from  
589 participants in the multiple-dose part of the study before dosing and at 0.5, 1, 1.5, and 2 hours  
590 after dosing on Days 1 and 14, as well as before dosing and 2 hours after dosing on Days 2,  
591 3, and 4. Because anti-SARS-CoV-2 IgY was not measurable at the time of the theoretical  
592 maximum serum concentration at 2 hours postdose on Day 14, the remaining postbaseline  
593 PK samples were not analyzed.

## 594 **Interim Analyses**

595 Before dose escalation in the single-ascending dose cohorts, the SMC was to review all available  
596 safety and tolerability data for a minimum of 7 participants who completed the planned safety  
597 assessments up to 48 hours after dosing. The SMC was composed of an independent medical  
598 monitor, principal investigator, and sponsor's medical representative. The data was to be  
599 reviewed blinded, unless the SMC considered it necessary to unblind the data for safety  
600 concerns. Before breaking the code per standard procedures, the potential decisions and actions  
601 were to be determined. SMC decisions on dose escalation were to be taken in consensus between  
602 the members of the SMC. The SMC decisions and their rationale were documented.

## 603 **Analyses**

604 No formal sample size calculations were done. Based on experience for previous similar studies,  
605 the target number of participants to be enrolled was appropriate for the assessment of safety,  
606 tolerability, and PK. The planned sample size was 48 participants. A total of 48 participants were  
607 enrolled and included in the safety analyses. The analysis of safety variables included all

608 participants who received study drug. All variables were summarized by descriptive statistics for  
609 each treatment group. The statistics for continuous variables included mean, median, standard  
610 deviation, and number of observations. Categorical variables were tabulated using frequencies  
611 and percentages. The incidence of all reported adverse events and treatment-related adverse  
612 events was tabulated by treatment group. Adverse events were also classified by system organ  
613 class and preferred term using the Medical Dictionary for Regulatory Activities. Adverse events  
614 were to be listed and summarized by treatment group, preferred term, severity, seriousness, and  
615 relationship to study drug. In the event of multiple occurrences of the same adverse events with  
616 the same preferred term in one participant, the adverse event was counted once as the worst  
617 occurrence. Summary statistics for actual values and change from baseline were analyzed for  
618 laboratory results by treatment group and scheduled visit. Data summarized by treatment  
619 included adverse events, vital signs, electrocardiogram parameters, and clinical laboratory  
620 evaluations.

## 621 **Cytokine measurement and analysis**

622 This non-GLP blinded assay was performed on sera of study participants by the Immunoassay  
623 Team at the Human Immune Monitoring Center at Stanford University (Stanford, CA), as  
624 described for the rat cytokine assay above. The levels of 80 different cytokines were determined.

## 625 **GLP bioanalytical analysis of IgY in blood samples – toxicokinetic analysis**

626 The presence of anti-SARS-CoV-2 IgY in sera of study participants was evaluated using GLP  
627 standards in a qualified ELISA assay at Charles River Laboratories (Reno, NV). ELISA 96-well  
628 plates were coated with goat anti-chicken IgY (Thermo Fisher; A16056) and, after blocking,  
629 were incubated with the samples containing anti-SARS-CoV-2 IgY at various concentrations for

630 1 hour at room temperature. After washing the microplate, rabbit anti-chicken IgY (Thermo  
631 Fisher; A16130) - HRP conjugate was added and incubated for 1 hour at room temperature. The  
632 ELISA plate was washed and substrate (3,3',5,5'-tetramethylbenzidine) was added to the wells  
633 and incubated for 20 minutes. The color development was stopped by the addition of 2N sulfuric  
634 acid and color intensity measured in a microplate reader at 450 nm. A calibration curve from the  
635 absorbance values was obtained from the standards using a 4-parameter curve fit with a  
636 weighting equation of  $1/y^2$ . The concentrations of anti-SARS-CoV-2 IgY in the samples were  
637 determined from the calibration curve. After 4 analytical method validations, lower and upper  
638 limit of detection, intra- and inter-assay precision and accuracy, dilution integrity, and short-term  
639 stability, IgY levels in study participants before and after 14 days of treatment were below the  
640 limit of detection.

## 641 **Good Laboratory Practice**

642 The study was performed at Charles River Laboratories following the U.S. Department of Health  
643 and Human Services, Food and Drug Administration (FDA), United States Code of Federal  
644 Regulations, Title 21, Part 58: Good Laboratory Practice for Nonclinical Laboratory Studies and  
645 as accepted by Regulatory Authorities throughout the European Union (OECD Principles of  
646 Good Laboratory Practice), Japan (MHLW), and other countries that are signatories to the  
647 OECD Mutual Acceptance of Data Agreement.

## 648 **Animal welfare assurance and standards**

649 The protocols and any amendment(s) or procedures involving the care and use of animals (hen  
650 immunization and rat tolerability studies) were reviewed and approved by Charles River  
651 Laboratories Institutional Animal Care and Use Committee before conduct. The hamster efficacy  
652 study was carried out following the recommendations in the Guide for the Care and Use of

653 Laboratory Animals of the National Institutes of Health and the protocol was approved by the  
654 Institutional Animal Care and Use Committee at the Washington University School of Medicine  
655 (assurance number A3381–01). Stanford Institutional Animal Care and Use Committee did not  
656 review the research.

## 657 **Regulatory and ethics considerations**

658 Ethical review of the clinical trial protocol and any amendments was obtained by Bellberry  
659 Human Research Ethics Committee (the Australian National Review Board) and the clinical trial  
660 was conducted solely at Linear Clinical Research, Perth Australia. Stanford Institutional Review  
661 Board did not review the research. The study was conducted following the protocol and ethical  
662 principles stated in the 2013 version of the Declaration of Helsinki and the applicable guidelines  
663 on Good Clinical Practice, and all applicable federal, state, and local laws, rules, and regulations.

## 664 **Results**

### 665 **Antigen production**

666 The overall scheme describing the production of anti-SARS CoV-2 IgY antibody to be used as  
667 intranasal prophylaxis in humans is shown in Figure 2A. We produced a recombinant protein to  
668 immunize hens. A tagless RBD of SARS-CoV-2 (Fig. 2B; index SARS-CoV-2 variant), amino  
669 acids 328-533, was produced in a cell-free protein synthesis reaction using *E.coli* extract  
670 [19,20,26]. Analysis of the purified CoV-2 RBD protein yielded a single protein band with an  
671 apparent molecular weight of 23 kDa (Fig. 2C). The purified SARS-CoV-2 RBD was eluted as a  
672 single peak by analytical size-exclusion chromatography with >95% monomer content (Fig. 2C).  
673 Bacterial endotoxin contamination was determined to be <0.1 EU/mg by Charles River Endosafe  
674 LAL cartridge system.

675 Integrity of the cell-free (non-glycosylated) SARS-CoV-2 RBD was then verified by  
676 kinetic binding to the hACE2 receptor. Binding kinetics and affinity were similar to a  
677 mammalian expressed and glycosylated S1 fragment (Fig. 2D) and were consistent with  
678 previously described binding affinities, suggesting the RBD expressed cell-free was properly  
679 folded and bioactive.

680 **Figure 2. RBD and IgY preparation.** (A) Workflow of the study. IgY preparation for  
681 intranasal drops as antiviral prophylaxis. (B) Cell-free expressed RBD derived from the Spike  
682 protein on the viral envelope of SARS-CoV-2. (C) Characterization of the recombinant protein  
683 RBD by ELISA and HPLC. (D) Determination of the affinity of the cell-free expressed RBD  
684 (amino acids 328-533) and mammalian-expressed full-length S1 to the hACE2 using Biacore.

## 685 **Hen immunization with SARS-CoV-2 RBD and IgY**

### 686 **characterization in vitro**

687 Cell-free expressed RBD (Fig. 2B; 50 µg in simple oil emulsion) was injected into 9 SPF hens  
688 (46-weeks old) and IgY was extracted from egg yolks using a water-based method 2 weeks after  
689 the second immunization and thereafter. The IgY preparation was subjected to protein and  
690 Western blot analyses (Fig. 3A). The IgY preparations were >95% pure; a quantitative Western  
691 blot analysis demonstrated that this preparation contained less than 2% ovalbumin by weight  
692 (Fig. 3A). Chromatography of the IgY preparations on size-exclusion HPLC identified 5 peaks  
693 (Fig. 3B); SDS-PAGE and Western blot analysis of the peaks collected between 17 and 30  
694 minutes confirmed that these peaks all contain IgY. The anti-SARS-CoV-2 RBD IgY antibodies  
695 recognized both the immunogen, cell-free expressed RBD, and the mammalian-expressed full-  
696 length and glycosylated S1 protein (Fig. 3C). One egg yolk of the SPF hens provided about 500  
697 mg of purified IgY and each of >10 independent batches of IgY, purified from 100 eggs, each

698 yielded an average of  $47 \pm 13$  g (SD) of purified IgY (Fig. 3D). There was limited variability in  
699 the affinity of the various IgY batches for the S glycosylated protein as judged by ELISA (Fig.  
700 3D; average titer against full-length S1 was 1:18,000). Furthermore, there was almost no  
701 difference in titer of individual hens towards the full-length glycosylated S protein, suggesting  
702 minimal variability between hens (Fig. 3E, F). Over 11 months, IgY was collected in batches of  
703 100 eggs per preparation with a similar yield of IgY per preparation and a similar response;  
704 interruption of immunization for 3 months did not result in a drop in titer (Fig. 3F, right panel).  
705 Approximately 300  $\mu\text{g}/\text{mL}$  IgY provided 50% neutralization of the index virus in culture (Fig.  
706 3H).

707 **Figure 3. IgY purification and characterization.** (A) Western blot analysis of the IgY  
708 preparation. (B) HPLC profile of the IgY preparation. (C) Western blot analysis of anti-SARS-  
709 CoV-2 IgY against RBD fragment and full S1 recombinant protein. (D) IgY yield for various  
710 batches derived from 100 eggs each. (E) Western blot data of different lots of anti-SARS-CoV-2  
711 RBD IgY (Y0120-Y0199). Pools of 100 eggs laid by 9 hens over 2 weeks were used for each  
712 pool of IgY preparation between May 2020 and March 2021. IgY lot samples were diluted 1:500  
713 followed by a 1:3000 dilution of rabbit anti-IgY HRP conjugate. First left lane shows the  
714 Coomassie stain of the same gels. (F) Time-dependent ELISA titers of sera from 3 individual  
715 hens following continual immunization (left); arrows indicate immunization timing. Time-  
716 dependent ELISA titer of 3 hens after immunization was stopped for up to 12 weeks (right). (H)  
717 Neutralization of pseudovirus SARS-CoV-2 by various lots of anti-SARS-CoV-2 RBD IgY  
718 (conducted at RetroVirox). (I) Neutralization of live index SARS-CoV-2 virus by anti-SARS-  
719 CoV-2 RBD IgY (Y0180, conducted at USAMRIID).



## 720 **Neutralization of SARS-CoV-2 index strain and variants of interest** 721 **and concern with anti-SARS-CoV-2 RBD IgY**

722 Pseudoviruses are synthetic chimeras that consist of a surrogate viral core derived from a parent  
723 virus and an envelope glycoprotein derived from a heterologous virus [26]. Viral neutralization  
724 assays in culture (RetroVirox) used non-replicative VSV pseudoviruses carrying a firefly  
725 luciferase reporter gene and expressing S of SARS-CoV-2 on the surface of the virion (VSV-S).  
726 The neutralization assay was performed with HEK 293T-hACE2, a human embryonic kidney  
727 cell line overexpressing hACE2, the receptor of the SARS-CoV-2 virus. First, 5 batches of RBD  
728 IgY preparations were tested. The neutralization activity of the purified IgY, defined as the  
729 concentration inhibiting 50% of the viruses ( $IC_{50}$ ) was  $\sim 170 \mu\text{g/mL}$  (Fig. 3G). Importantly,  $\sim 10$ -  
730 fold higher neutralization activity towards the index SARS-CoV-2 virus was observed when  
731 using a live index virus (Fig. 3H).

732 Because at least 13 common variants of SARS-CoV-2 with amino acid mutations in the  
733 RBD had emerged since December 2020 [27-29] (Fig. 4A), we tested the activity of the anti-  
734 SARS-CoV-2 IgY against several variants (including Beta, Delta, and Omicron; Fig. 4A, B) and  
735 D614G, an amino acid substitution outside the RBD that is now found in most variants. Beta,  
736 Delta, and Omicron were classified as variants of concern, associated with increased  
737 transmissibility or detrimental change in COVID-19 epidemiology, or an increase in virulence or  
738 change in clinical disease presentation.

739 First, IgY antibody ELISA titer against Beta RBD was compared with the RBD of the  
740 index SARS-CoV-2 virus as well as the most common Alpha variant. ELISA with recombinant  
741 full-length S protein or the RBD of the 3 mutants as well as the immunizing RBD fragment of  
742 the index virus yielded a virtually identical titer (Fig. 4C). Although the Omicron variant still

743 uses the hACE2 receptor to infect human cells [10,30], the RBD contains a total of 15 mutations  
744 compared to the index virus, 11 of which were not found in the previous variants (Fig. 4A, B).  
745 Yet, the ELISA titer of IgY against the Omicron RBD was also equivalent or slightly better than  
746 that towards the RBD of the index virus (Fig. 4D).

747         Next, we tested the neutralization titer of anti-SARS-CoV-2 RBD IgY (lot Y0180)  
748 against the RBD of the index, Alpha, and Beta variants, thus including all the amino acid  
749 substitutions within the RBD also found in the RBD of Gamma, Zeta, Eta, Theta, Iota, and Mu  
750 variants and 1 of the 2 substitutions in the Kappa variant (Fig. 4A). The IC<sub>50</sub> of the VSV-S  
751 pseudovirions for the index strain and Beta variant were virtually identical: 668 µg/mL for the  
752 index strain, 568 µg/mL for Beta (Fig. 4E), and 2-fold lower for Alpha (IC<sub>50</sub> = 302 µg/mL; Fig.  
753 4E). RetroVirox also provided data using plasma from a single Moderna-vaccinated individual  
754 for a titer comparison of neutralization with anti-SARS-CoV-2 RBD IgY, tested with 3 of the  
755 variants. In a side-by-side study, the IC<sub>50</sub> generated with the human plasma from a recipient of  
756 the mRNA Moderna vaccine (2 doses; index SARS-CoV-2) showed the highest titer against the  
757 index virus, followed by a 2.8-fold drop in titer towards Alpha and a 6.7-fold lower titer for Beta  
758 (Fig. 4F).

759         The anti-SARS-CoV-2 IgY preparation was similarly effective against the Delta variant  
760 compared with the index strain (Fig. 4G). The assays show that Y0180 displays similar  
761 neutralizing activity against both isolates; IC<sub>50</sub> values generated were 635 µg/mL (Delta) and 739  
762 µg/mL (index virus). Plasma from a Moderna-vaccinated individual was also tested in parallel  
763 with both isolates. NT<sub>50</sub> values generated with this plasma against the variants were 1:1274  
764 (Delta pseudovirus) and 1:1091 (index pseudovirus). The neutralization activities of the antibody  
765 and control plasma against both variants were also confirmed by microscopy evaluating the

766 virus-induced CPE in infected cell monolayers (Fig. 4H). The human serum had a similar degree  
767 of neutralization against the index pseudovirus and Delta (Fig. 4H) when tested at a dose that is  
768 three times higher than that required for 50% neutralization (1:640 in Fig. 4H, middle panels, vs.  
769 1:2,000 in Figure 4F). In contrast, anti-SARS-CoV-2 IgY tested at 400  $\mu\text{g}/\text{mL}$  (Fig. 4H, right  
770 panels), a dose below that required for 50% neutralization ( $\sim 650 \mu\text{g}/\text{mL}$ ; Fig. 4G), was equally  
771 effective against both variants. Together, these data indicate that the spectrum of the polyclonal  
772 anti-SARS-CoV-2 RBD IgY displays sufficient diversity so that none of the common point  
773 mutations in the RBD associated with a greater transmission rate of the virus affected the  
774 neutralization efficacy of these most common SARS-CoV-2 variants of concern.

775 **Figure 4. Common variants of SARS-CoV-2 and anti-SARS-CoV-2 IgY interaction**  
776 **with them.** (A) A scheme depicting locations of mutated amino acids in Alpha through Mu  
777 variants of SARS-CoV-2, focusing on the RBD domain only. Each color bar indicates the amino  
778 acid in the index virus that was mutated in the variant. (B) Spike protein of SARS-CoV-2 Alpha,  
779 Beta, Delta, and Omicron are shown from left to right. Molecular Operating Environment was  
780 used to create the figure [31]. The location of mutations in the structure of the S protein trimer of  
781 SARS-CoV-2 (PDB ID: 7A98) for 4 of the common variants are indicated in red and  
782 glycosylation sites are indicated in pink throughout the S protein. Blue ribbon indicates RBD  
783 (amino acids 328-533) and the orange ribbon indicates receptor binding motif (amino acids 437-  
784 508). (C) Binding of anti-SARS-CoV-2 RBD IgY to recombinant S1 full length (FL) of the  
785 index virus, the RBD of the Alpha and Beta variants, and the immunizing RBD of the index  
786 virus by ELISA. (D) Binding of anti-SARS-CoV-2 RBD IgY to the index virus and Omicron  
787 variant (B.1.1.529) RBD domain using ELISA. (E) Neutralization of pseudovirus (VSV-S)  
788 SARS-CoV-2 carrying S protein of index pseudovirus, Alpha, or Beta variants by anti-SARS-

789 CoV-2 RBD IgY. (F) Neutralization of pseudoviruses listed in (E) by Human anti-SARS-CoV-2  
790 RBD. (G) Neutralization of live index or Delta viruses by anti-SARS-CoV-2 IgY against the  
791 RBD. (H) Neutralization of live D614G vs. Delta variants by human serum of immunized  
792 individual or by anti-SARS CoV-2 IgY. Microscopic evaluation of monolayers of Vero E6 cells  
793 after 96 hours infection with the indicated authentic (live) SARS-CoV-2 variant. Images from  
794 infected cells are shown after 4 days of infection with SARS-CoV-2 variants in the absence or  
795 presence of test items. Top three panels: Infection in the presence of MEX-BC2/2020 and bottom  
796 three panels: infection with the Delta variant each in the presence of vehicle alone, serum of a  
797 person immunized twice with the Moderna (mRNA-1273) vaccine or anti-SARS CoV-2 RBD  
798 IgY, as indicated, all at the indicated concentration (neutralization experiments in panels E-H  
799 were conducted by RetroVirox using pseudovirus or live virus, as indicated). Except when  
800 indicated, the studies were done over several months; therefore, the absolute titers in the ELISA  
801 and neutralization studies were not identical. However, each experiment included the same  
802 positive control; index RBD for ELISA and index virus for neutralization assays.

### 803 **Efficacy study in a hamster model of COVID-19**

804 We did not find in vivo efficacy of anti-SARS-CoV-2 RBD IgY in the Syrian golden hamster  
805 COVID-19 model against a challenge with a titer of 0.8 or  $4 \times 10^6$  of SARS-CoV-2 virus, likely  
806 because the amount of virus we employed was too high. Lung viral load after 3 days was  
807 comparable between the control treatment group and the anti-SARS-CoV-2 RBD IgY treatment  
808 group, but body weight loss was more severe in control animals (S1 Fig).

### 809 **Rat toxicity and safety study**

810 All 8-week-old Sprague Dawley rats (10 males and 10 females) in the 28-day GLP safety study  
811 (Fig. 5A) survived to scheduled euthanasia with no mortality, test article-related organ weight  
812 changes, or gross or microscopic findings (see Fig. 5B). There were also no differences between

813 female and male groups in each treatment arm. The GLP-qualified assay detected no anti-SARS-  
814 CoV-2 RBD IgY in the sera of animals after 28 days of daily treatment with 4 mg anti-SARS-  
815 CoV-2 RBD IgY (lower limit of detection of 30 ng/mL).

816           There was no evidence of significant systemic immune activation in the rats (20/group)  
817 treated as above by measuring changes in levels of 27 proinflammatory serum cytokines after  
818 anti-SARS-CoV-2 RBD IgY administration (Fig. 5C). When comparing posttreatment (Day 1 at  
819 4 hours and Day 28 at 24 hours after twice-daily treatments) to pretreatment serum levels (Day 1,  
820 time 0; D1 H0), there were no changes for most of the cytokines (22 of the 27 tested) in both  
821 placebo- and IgY-treated groups at any time. Compared with D1 H0, we detected a transient,  
822 slight increase in interleukin-1 (IL-1) beta and monocyte chemoattractant protein-1 (MCP1) on  
823 Day 1, 4 hours after anti-SARS-CoV-2 RBD IgY administration. A similar trend that did not  
824 reach significance was also observed in the placebo group at the same time; increases in IL-1  
825 beta and MCP1 were not seen at any other time. There was a significant increase in interferon-  
826 inducible protein 10 (IP10) on Day 1, 4 hours after the first treatment compared to D1 H0,  
827 observed in both treatment and placebo group. A significant decrease in D1 H24 in the placebo  
828 arm was observed only for RANTES (Fig. 5C). Nonetheless, none of these changes in cytokines  
829 were observed in the rats at other time points. Together, our data show that long-term twice-daily  
830 administration of 4 mg/mL IgY (or 16 mg/kg) up to 28 days in rats has excellent safety and  
831 tolerability with no evidence of systemic immune activation.

832           **Figure 5. Preclinical toxicity of 28-day treatment with anti-SARS-CoV-2 RBD IgY**  
833 **in rats.** (A) Study design. (B) Summary of findings. (C) Serum levels of 27 cytokines over time  
834 in rats treated with IgY (Tx) or vehicle/placebo (PL). Data are provided for Day 1 before  
835 treatment (D1H0); Day 1, 4 hours after the treatment (D1H4); 24 hours after the two treatments,

836 6 hours apart, at 24 hours after the first treatment (D1H24); 28 days of twice-daily treatments  
837 and 4 hours of the treatment of that day (D28H4); and 28 days of twice-daily treatments and 24  
838 hours of the treatment of that day (D28H24). Red indicates a statistical difference with a false  
839 discovery rate (FDR) significant p-value ( $p < 0.05$ ).

## 840 **Human tissue cross-reactivity study**

841 We determined potential cross-reactivity of the anti-SARS-CoV-2 RBD IgY protein to a full  
842 panel of human tissues (at least 3 donors per tissue; see S4 Table for a list of human tissues  
843 tested for reactivity). Anti-SARS-CoV-2 RBD IgY reactivity at two concentrations (20 and 10  
844  $\mu\text{g/mL}$ ) was compared with control polyclonal chicken IgY antibodies (negative control), and  
845 with anti-human macroglobulin (positive control for staining). No specific binding was observed  
846 with the anti-SARS-CoV-2 RBD IgY to any of the human tissue panels examined, including  
847 human nasal cavity and lung (see Fig. 6).

848 **Figure 6: Lack of cross-reactivity of anti-SARS-CoV-2 RBD IgY with human**  
849 **tissues.** Immunohistochemical testing of anti-SARS-CoV-2 RBD IgY (top row), control IgY  
850 (middle row; negative control), and anti-human macroglobulin antibodies (bottom row; positive  
851 control) with human nasal mucosa (left two panels) and human lungs (right two panels). Bars  
852 provide a magnification scale.

## 853 **Phase 1 Clinical Trial Results**

854 Forty-seven of 48 enrolled participants completed the study drug treatment period and planned  
855 study visits. One participant in the multiple-dose part was withdrawn from the study after  
856 receiving 3 doses (Day 1) of placebo due to a concurrent upper respiratory tract infection, judged  
857 to be unrelated to study drug by the investigator.

## 858 **Baseline Demographics**

859 Study participants ranged in age from 20 to 43 years (median, 25.5) in the single-dose part of the  
 860 study and 18 to 40 years (median, 23.0) in the multiple-dose part (Tables 1,2). Female  
 861 participants comprised 75% of the population in the single-dose study segment and 46% in the  
 862 multiple-dose study segment. Demographics are summarized in Tables 1 and 2.

863 **Table 1. Demographics of participants in single-ascending dose group (Part 1).**

864

Anti-SARS-CoV-2 IgY					All Participants N=24
	2 mg N=6	4 mg N=6	8 mg N=6	Placebo N=6	
<b>Age, years</b>					
Mean (SD)	28.8 (7.99)	27.3 (4.76)	27.7 (5.65)	22.7 (2.34)	26.6 (5.72)
Median (range)	26.5 (20-43)	28.0 (21-33)	27.5 (20-37)	22.0 (20-27)	25.5 (20-43)
<b>Gender, n (%)</b>					
Female	4 (66.7)	4 (66.7)	4 (66.7)	6 (100)	18 (75.0)
Male	2 (33.3)	2 (33.3)	2 (33.3)	0	6 (25.0)
<b>Ethnicity, n (%)</b>					
Hispanic or Latino	1 (16.7)	0	0	0	1 (4.2)
Not Hispanic or Latino	5 (83.3)	6 (100)	6 (100)	6 (100)	23 (95.8)
<b>Race, n (%)</b>					
Asian	2 (33.3)	1 (16.7)	0	0	3 (12.5)
Native Hawaiian or Other Pacific Islander	0	0	0	1 (16.7%)	1 (4.2%)
White	4 (66.7)	5 (83.3)	6 (100)	5 (83.3)	20 (83.3)

865

866 **Table 2: Demographics of participants in the multiple-dose group (Part 2).**

Anti-SARS-CoV-2 IgY					All Participants N=24
	2 mg TID N=6	4 mg TID N=6	8 mg TID N=6	Placebo TID N=6	
<b>Age, years</b>					
Mean (SD)	26.0 (8.37)	21.8 (2.14)	27.5 (6.92)	25.3 (6.41)	25.2 (6.33)
Median (range)	23.0 (18-40)	22.0 (19-25)	25.0 (21-37)	25.0 (18-36)	23.0 (18-40)
<b>Gender, n (%)</b>					
Female	1 (16.7)	4 (66.7)	2 (33.3)	4 (66.7)	11 (45.8)
Male	5 (83.3)	2 (33.3)	4 (66.7)	2 (33.3)	13 (54.2)
<b>Ethnicity, n (%)</b>					
Hispanic or Latino	0	0	1 (16.7)	1 (16.7)	2 (8.3)
Not Hispanic or Latino	6 (100)	6 (100)	5 (83.3)	5 (83.3)	22 (91.7)

**Race, n (%)**

Asian	1 (16.7)	2 (33.3)	2 (33.3)	2 (33.3)	7 (29.2)
Black or African American	0	0	0	1 (16.7)	1 (4.2)
White	5 (83.3)	4 (66.7)	4 (66.7)	3 (50.0)	16 (66.7)

867 tid = 3-times daily

868 **Safety and tolerability**

869 The overall incidence of treatment-emergent adverse events was 29% (7 of 24 participants; Table  
 870 3) in the single-dose part of the study and 58% (14 of 24 participants; Table 4) in the multiple-  
 871 dose part of the study, with similar incidence rates between anti-SARS-CoV-2 RBD IgY (42%)  
 872 and placebo (50%) groups (Tables 3, 4). The most frequent treatment-emergent adverse event  
 873 was headache, with similar rates between placebo (17%) and anti-SARS-CoV-2 RBD IgY (14%)  
 874 (Tables 3,4).

875 **Table 3. Adverse events by preferred term- single ascending-dose study (Part 1).**

	Anti-SARS-CoV-2 IgY					All Participants (N=24) n (%) E
	2 mg (N=6)	4 mg (N=6)	8 mg (N=6)	Placebo (N=6)		
	n (%) E	n (%) E	n (%) E	n (%) E		
Participants with $\geq 1$ TEAE	1 (16.7%) 1	2 (33.3%) 2	2 (33.3%) 2	2 (33.3%) 2	7 (29.2%) 7	
<b>MedDRA Preferred Term</b>						
Fatigue	0	0	1 (16.7%) 1	1 (16.7%) 1	2 (8.3%) 2	
Erythema	0	0	1 (16.7%) 1	0	1 (4.2%) 1	
Headache	0	1 (16.7%) 1	0	0	1 (4.2%) 1	
Sneezing	0	1 (16.7%) 1	0	0	1 (4.2%) 1	
Tension headache	1 (16.7%) 1	0	0	0	1 (4.2%) 1	
Thermal burn	0	0	0	1 (16.7%) 1	1 (4.2%) 1	

876 E = number of events; n = number of participants; TEAE = treatment-emergent adverse event

877

878 **Table 4. Adverse events by preferred term- multiple-dose study (Part 2).**

	Anti-SARS-CoV-2 IgY				All Participants (N=24)
	2 mg TID (N=6)	4 mg TID (N=6)	8 mg TID (N=6)	Placebo TID (N=6)	



	n (%) E	n (%) E	n (%) E	n (%) E	n (%) E
Participants with $\geq 1$ TEAE	4 (66.7%) 7	2 (33.3%) 3	4 (66.7%) 5	4 (66.7%) 5	14 (58.3%) 20
<b>MedDRA Preferred Term</b>					
Headache	0	0	3 (50.0%) 3	2 (33.3%) 2	5 (20.8%) 5
Upper respiratory tract infect	0	0	1 (16.7%) 1	1 (16.7%) 1	2 (8.3%) 2
Contusion	0	0	0	1 (16.7%) 1	1 (4.2%) 1
Dental discomfort	1 (16.7%) 1	0	0	0	1 (4.2%) 1
Dizziness	1 (16.7%) 1	0	0	0	1 (4.2%) 1
Ear pain	1 (16.7%) 1	0	0	0	1 (4.2%) 1
Epistaxis	1 (16.7%) 1	0	0	0	1 (4.2%) 1
Eyelid irritation	0	0	1 (16.7%) 1	0	1 (4.2%) 1
Injection site haematoma	1 (16.7%) 1	0	0	0	1 (4.2%) 1
Nasal congestion	0	0	0	1 (16.7%) 1	1 (4.2%) 1
Parosmia	0	1 (16.7%) 1	0	0	1 (4.2%) 1
Presyncope	1 (16.7%) 1	0	0	0	1 (4.2%) 1
Rhinorrhoea	0	1 (16.7%) 1	0	0	1 (4.2%) 1
Skin abrasion	0	1 (16.7%) 1	0	0	1 (4.2%) 1
Tenderness	1 (16.7%) 1	0	0	0	1 (4.2%) 1

879 E = number of events; n = number of participants; TEAE = treatment-emergent adverse event

880

881 All adverse events were mild (grade 1) in severity. No serious adverse event or lab-  
882 related adverse event was reported, and there was no dose dependency of adverse events  
883 observed. Furthermore, no participant receiving anti-SARS-CoV-2 RBD IgY had an adverse  
884 event of nasal irritation or nasal congestion. There were no clinically significant observations or  
885 trends noted in laboratory assessments, vital signs, physical exam findings, or electrocardiograms  
886 during the study.

### 887 **Pharmacokinetics**

888 PK analyses indicated no evidence of serum anti-SARS-CoV-2 RBD IgY above the lowest  
889 detection levels of 30 ng/mL (using a GLP study at Charles River Laboratories) in the 18  
890 participants who received anti-SARS-CoV-2 RBD IgY in the multiple-dose part of the study.

### 891 **Serum cytokines**

892 Levels of 80 different cytokines in sera of 19 participants of the multiple-dose part were

893 tested before treatment (D1 pre-dose), 2 hours after dosing on day 1 (D1 H2); day 2, before  
894 treatment (D2 pre-dose), and 2 hours after the first dosing on day 2 (D2 H2, Fig. S2). There were  
895 slight but statistically significant decreases (red histograms) in 10 of the 80 cytokines (Fig. S2).  
896 These slight declines in CCL27, CXCL9, IL23, IL27, LIF, MIP5, RESISTIN, TNF $\alpha$ , TNF $\beta$ , and  
897 TNFRSF6 were noted only in the 12 mg/day group compared to the pretreatment levels (Fig.  
898 S2). These declines also occurred only 2 hours after the first dose (D1 H2) and were not  
899 sustained, except for MIP5 (Fig. S2). There was also a small decrease in IL3, 2 hours after the  
900 first dose of 6 mg/day group anti-SARS-CoV-2 RBD IgY, but there were no changes in this  
901 cytokine at any other times or doses (Fig. S2). These slight changes, which were also not  
902 sustained or dose dependent, were judged to be artifactual. Overall, there were no clinically  
903 relevant increases in serum cytokines at any time for any of the treatment groups (6, 12, or 24 mg  
904 total daily dose of anti-SARS CoV-2 RBD IgY for 14 days).

## 905 **IgE and anti-IgE**

906 The anti-SARS-CoV-2 IgY preparation contains ovalbumin. Although participants with egg  
907 allergies were excluded from the trial, an exploratory analysis was conducted of pretreatment  
908 serum total IgE and anti-IgE antibody (mainly anti-ovalbumin) levels in the 24 participants in the  
909 multiple-dose part of the trial. No participant had detectable serum egg-white specific IgE  
910 antibodies (all <0.35 kU/L).

## 911 **Discussion**

912 Despite recent successes in generating highly effective COVID-19 vaccines, there is an ongoing  
913 need for widely available and safe antiviral strategies that reduce infection and transmission  
914 worldwide. Limitations to current vaccines include global vaccine availability and affordability,  
915 vaccine hesitancy, and rapidly emerging highly infective viral strains that escape vaccine-

916 induced immunity. This has been particularly apparent following the emergence of Delta and  
917 Omicron. The latter variant was first detected in specimens collected on November 8, 2021 [32],  
918 and within a few weeks became the dominant SARS-CoV-2 variant in the United States [33].  
919 Both convalescent sera from early strain-infected patients and fully vaccinated individuals  
920 exhibited a low neutralization capacity against Omicron [9-12]; a reduction of 30 to 40-fold in  
921 neutralization titers was reported. Furthermore, of eight currently authorized or approved  
922 monoclonal antibodies, seven did not neutralize the Omicron variant and one had a 3-fold  
923 reduction in neutralization titer [11]. These data highlight the need for alternative and  
924 complementary approaches to curb COVID-19.

925         Here, we describe the production of the first chicken egg yolk-derived anti-index SARS-  
926 CoV-2 RBD IgY polyclonal antibodies as an intranasal drop product for humans with equal in  
927 vitro activity against all variants of concern. These IgY were raised in SPF hens and showed an  
928 excellent safety profile when given intranasally by drops to rats for 28 days (4 mg/day). No  
929 toxicity, innate inflammatory response, or systemic exposure to IgY were noted in this GLP  
930 study. In 48 healthy adult participants, anti-SARS-CoV-2 RBD IgY given intranasally at single-  
931 ascending doses of 2, 4, and 8 mg and as total daily doses of 6, 12, and 24 mg for 14 days also  
932 had a highly favorable safety and tolerability profile. Importantly, no participant receiving  
933 intranasal anti-SARS-CoV-2 IgY in the multiple-dose phase had measurable levels of anti-  
934 SARS-CoV-2 RBD IgY in their sera, reflecting the absence of systemic absorption of topically  
935 administered IgY following intranasal application. We also found no evidence of a systemic  
936 inflammatory immune response triggered by the topical treatment with anti-SARS-CoV-2 RBD  
937 IgY in humans, and no detectable increase in 80 sera cytokines.

938 Hen-derived IgY antibodies have several advantages for topical use in humans; these  
939 antibodies do not bind the Fc receptor or rheumatoid factor or activate the human complement  
940 cascade [34], thus greatly reducing the risk of severe immune responses. These features support  
941 the clinical applications of IgY for nasal treatment in a wide range of persons, including the  
942 elderly, immunocompromised, and children. IgY has been beneficial with favorable safety and  
943 tolerability when given prophylactically in both animal models and clinical settings of viral  
944 diseases, including respiratory infections (reviewed in [35]). Overall, available data to date  
945 suggest that IgY given by nonparenteral administration does not have unwanted off-target  
946 proinflammatory effects and is nontoxic to humans, thus permitting potential clinical  
947 applications in diverse populations and diseases.

948 The potential use of IgY from hens immunized with inactivated virus [36], full length  
949 recombinant S protein [37-40], or N protein [41] has been explored with studies evaluating  
950 neutralization of the virus in cells, with IC<sub>50</sub> values of 10 mg/mL [36], 1 mg/mL [37], 16.8  
951 mg/mL [38], and 0.27 mg/mL [39]. However, the ability of these egg-derived antibodies to  
952 neutralize other common SARS-CoV-2 variants has not been evaluated and their safety profile in  
953 animals or humans has not been assessed.

954 Intranasally administered proteins are removed from the mucosal surface through ciliary  
955 movement [37, 42], which was the basis for using a 3-times daily (every 4 hours) regimen in our  
956 phase 1 study. The anti-SARS-CoV-2 RBD IgY was designed to capture and immobilize SARS-  
957 CoV-2 on the nasal mucosa, preventing the virus from binding to and spreading across the nasal  
958 mucosa, and also preventing the transmission of the virus to other individuals. Intranasal delivery  
959 of mammalian immunoglobulins as antiviral agents has been extensively tested in humans [43-  
960 48]. Human immunoglobulins G (IgG) and A (IgA) given intranasally are well tolerated [43-48],

961 including in pediatric populations. Our decision to protect from viral entry at the nasal mucosa  
962 stems from the observation that levels of lung hACE2 are much lower than in the nose; infection  
963 of lung tissue is >5 orders of magnitude lower compared with nasal mucosa [49,50]. Therefore,  
964 inhibition of viral entry at the nose is likely the correct target site for optimal efficacy.

965 Our product is egg-derived immunoglobulins, which could contain potentially antigenic  
966 residual chicken proteins. However, it is not indicated for those who are allergic to egg yolks.  
967 Note also that most humans are exposed to egg-derived antigens through their diet and are not  
968 allergic. Furthermore, anaphylaxis for those who consume eggs regularly is rare. However, the  
969 safety and tolerability of hen-derived IgY as intranasal treatment in humans have not been  
970 described despite their extensive use in a variety of routes in animals and aquaculture [35,51].

971 Several other studies have examined anti-COVID-19 intranasal prophylaxis, mostly in  
972 animal models [52-58]. These prophylaxes include polymer barriers, active vaccines, existing  
973 antiviral drugs, inhibitors of protease-induced activation of the virus, antiseptics, antimicrobial  
974 agents, and antibodies. Most relevant for comparison with our study is the use of neutralizing  
975 antibodies. In one study, intranasal treatment with a monoclonal human antibody (500 µg in 100  
976 µL/nare) 12 hours after infection in hamsters inoculated with  $5 \times 10^4$  median tissue culture  
977 infective dose (TCID<sub>50</sub>) of SARS-CoV-2 decreased clinical disease signs and improved recovery  
978 during 9 days of infection compared with control antibody-treated hamsters [58]. However, in  
979 contrast to our study, there was a substantial systemic exposure to the human antibody 24 hours  
980 after a single intranasal treatment with 2.5 mg; serum levels of the treated antibodies in that  
981 study were 210 ng/mL vs. below detection levels (30 ng/mL) in our study following  
982 administration of 4 mg IgY antibodies intranasally daily for up to 28 days. Therefore, the benefit  
983 of the treatment in their study [58] could have been due to neutralization of the virus that had

984 entered the body rather than blocking entry of the virus at the nasal mucosa. Similarly, a single  
985 intranasal monoclonal immunoglobulin M (IgM) antibody administration in a mouse model of  
986 COVID-19 was highly efficacious when mice were infected with  $10^4$  PFU [56]. Human IgM  
987 systemic exposure was also noted in mice treated with human IgM monoclonal antibody anti-  
988 SARS-CoV-2, although the study attributed the protection to the persistent presence of the  
989 antibody at the nasal cavity for over 48 hours based on fluorescent tag measurement [56]. Such  
990 long persistence of levels of IgM in the nasal cavity is at odds with other studies, including when  
991 using  $^{99m}\text{Tc}$ -labeled albumin particles or fluorescently labeled IgY antibodies that showed  
992 residence time of 2-4 hours [37]. If the long persistence is not an artifact of the method, it may  
993 suggest a unique benefit of IgM treatment as COVID-19 prophylaxis. Note, however, that with  
994 one exception [56], none of these studies assessed the cross-reactivity of antibodies against the  
995 variants.

996 Our work shows that, although the IgY was raised against the ancestral (index) strain  
997 RBD, the repertoire of the antibodies raised in hens was diverse and polyclonal so that binding  
998 affinities measured by ELISA for the single (Alpha), double (Delta), and triple amino acid (Beta)  
999 substitutions, or the Omicron variant with 15 amino acid substitutions in the RBD, were not  
1000 different from the affinity for the index RBD or full-length S protein (Fig. 4C, D). We then  
1001 confirmed that there was no difference between Alpha, Beta, and Delta variants, and the index  
1002 strain in a neutralization assay in culture using a VSV-S pseudovirus or live virus (Fig. 4E, G),  
1003 whereas a reduced neutralization activity of human serum was observed in side-by-side  
1004 experiments (Fig. 4F, H). The viral neutralization studies reported here were conducted by a  
1005 commercial provider (RetroVirox) and by an established laboratory at the USAMRIID, both

1006 comparing the results with either convalescent sera or an immunized human, for relative titer  
1007 evaluation.

1008 The culture neutralization titer of anti-SARS-CoV-2 RBD IgY is lower than the human  
1009 anti-SARS-CoV-2 sera (e.g., Fig. 4F vs. E). However, this may reflect the need for protease-  
1010 induced RBD exposure in the full-length S protein for binding by IgY, which might not occur  
1011 effectively in the culture model. A comparison of titer values between our product and sera from  
1012 an immunized person can also be calculated based on values of IgG levels in human sera (~15  
1013 mg/mL); a titer of 1:2,000 (Fig. 4F; dashed line) is equivalent to ~7 ug/mL or 100-fold higher  
1014 IgG titer than our IgY (Fig. 4E; ~600 ug/mL). However, as the dose of the IgY anti-SARS-CoV-  
1015 2 preparation in humans is planned to be 4 mg/dose, more important is the equal potency of the  
1016 IgY towards the various variants when used even at ~1/10 of the intended IgY dose (Fig. 4H).

1017 Another potentially important difference between our findings and the previously  
1018 published study is the antigen used to raise the antibodies. When expressed in mammalian cells,  
1019 the full-length S1 protein has at least 22 glycosylation sites per S monomer [59]. As glycosylated  
1020 amino acids are more immunogenic, the affinity of the human antisera may reflect binding to the  
1021 glycosylated determinants of the protein. However, as glycosylation sites in the S1 protein are  
1022 heavily mutated and new sites may be formed in many of the variants [28], immune reactivity  
1023 that is biased towards glycosylated sites may lead to loss of activity as the virus mutates. This  
1024 will not occur when the non-glycosylated RBD is used as the immunogen, as we have done in  
1025 our study using cell-free expressed RBD [20,21]. Supporting the negative impact of glycosylated  
1026 antigen, increased immunogenicity of protein antigens after removal of glycosylation sites has  
1027 been previously shown for hepatitis C virus envelope antigen-based vaccines [60]. Furthermore,  
1028 the apparent higher titer in the neutralization assay may be biased if the tested virus has the same

1029 glycosylation sites as that used as an immunogen in vaccinated individuals; many studies use the  
1030 original viral isolates rather than the common current variants.

1031 An important feature of our product is the ease of developing prophylaxis that can be  
1032 quickly and inexpensively produced. We found that 24 mg total daily dose (divided into three  
1033 equal doses) of intranasal anti-SARS-CoV-2 IgY for 14 days had an excellent safety profile in  
1034 humans; this daily dose represents ~1/20 of one egg of immunized SPF hen and ~1/5 of an egg  
1035 of commercial hen, underscoring that such an IgY dose is feasible for both production cost and  
1036 effort.

1037 There are some limitations to our studies. Our phase 1 clinical trial in healthy volunteers  
1038 was to assess initial safety, tolerability, and PK of anti-SARS-CoV-2 IgY and was not designed  
1039 to evaluate efficacy. In addition, we were unable to obtain in vivo data showing viral  
1040 neutralization (Fig. S1.). This may reflect using too much virus in this animal model of COVID-  
1041 19; our study used  $8 \times 10^5$  or  $4 \times 10^6$ , vs. 1 or  $5 \times 10^4$  TCID<sub>50</sub> [55,58]. In addition, our intranasal  
1042 formulated IgY preparation was viscous to obtain better delivery in humans. As hamsters are  
1043 obligatory nose-breathers, they may have blown out the formulated IgY. Finally, the virus that  
1044 was delivered in 50  $\mu$ L of liquid directly into each nare may have washed out some antibodies.  
1045 Another limitation in our study is that the neutralization studies comparing the hen IgY vs.  
1046 human sera were not comprehensive and included only 1 or 2 human samples. Nevertheless, our  
1047 study is the first to demonstrate the broad selectivity of anti-SARS-CoV-2 IgY against all the  
1048 current variants of concern and a favorable safety profile when used chronically as intranasal  
1049 drops in rats and humans.

1050 There are also several advantages for the use of IgY as prophylaxis against other  
1051 pathogens besides SARS-CoV-2 that cause disease in humans. As we noted above, IgY



1052 generation is inexpensive and fast; one egg of an SPF hen produces 20-80 daily doses (at 6  
1053 mg/dose) within 3 weeks from the first injection (1 week after the first boost). We found a  
1054 limited variability between individual immunized hens as determined by ELISA and Western  
1055 blot analyses and a batch-to-batch consistency (Fig. 3D-G.). IgY is also easy to distribute;  
1056 besides the known long-term stability of purified IgY [61], we also found excellent stability of  
1057 the formulated material at 2-8°C for at least 6 months (maximum time point measured so far) and  
1058 greater than 2 weeks when stored at room temperature. This is in contrast to vaccines, some of  
1059 which require cold-chain storage at -80°C that complicates the logistics of global distribution and  
1060 to resource-poor regions, in particular.

1061 Another important advantage of IgY-based prophylaxis is the ease of local production,  
1062 including in low- and middle-income countries. As hen immunization is a standard procedure  
1063 around the world, IgY purification and formulation do not require expensive equipment and are  
1064 simple to carry out. In a separate study, we determined that the production of anti-SARS-CoV-2  
1065 antibodies against the same immunogen using commercial hens and the resulting IgY had very  
1066 similar activities to that of SPF hens, although the amount of IgY produced per egg was lower. In  
1067 addition, both the immunized hens and their eggs are safe for humans, even for consumption as  
1068 food, making the production of this prophylaxis easy to adopt in non-specialized facilities in  
1069 low-income countries. Therefore, anti-SARS-CoV-2 IgY can be readily made available  
1070 worldwide as an additional means of reducing SARS-CoV-2 infection. Each day, one immunized  
1071 hen can produce the daily dose required for prophylaxis of a family. In addition, by reducing  
1072 viral mobility and anchoring the virus to the nasal mucus, transmission of the virus from infected  
1073 to healthy individuals may be reduced.

## 1074 **Conclusion**

1075           The current COVID-19 pandemic illustrates the need for prophylactics that can be  
1076 produced rapidly at low cost, are technically accessible anywhere in the world, and complement  
1077 traditional vaccine development. The safety and benefit of IgY and the ease to produce it at low  
1078 cost are well described for animal farms. In contrast, the clinical adaptation of IgY for human use  
1079 has been slow, likely hampered by a lack of intellectual property that has hindered commercial  
1080 development by industry. For that reason, we undertook the effort of establishing the ability of  
1081 anti-SARS-CoV-2 IgY to neutralize variants of concern and the initial safety of the IgY  
1082 preparation using industry GLP and GMP standards. We suggest that until vaccination that is  
1083 highly effective against prevalent variants becomes available worldwide or herd immunity is  
1084 achieved, intranasal delivery of anti-SARS-CoV-2 IgY may provide passive immunization,  
1085 including for use as an add-on to personal protective equipment and other preventive measures  
1086 for the general population. This IgY may also provide short-term protection in addition to  
1087 vaccines in less well-ventilated environments, including in trains, airplanes, lecture halls, etc. We  
1088 also suggest that this approach has the potential to provide a means to curb new threats of  
1089 epidemics by airborne infectious agents; by providing the relevant immunogen for hen  
1090 immunization at the geographical site where the threat was detected, an effective passive  
1091 immunity can be initiated locally to stop the spread of the airborne infectious agent before it  
1092 becomes an epidemic. We hope that this study will trigger further work to evaluate the safety and  
1093 efficacy of anti-SARS-CoV-2 IgY in those at risk of SARS-CoV-2 infection.

## 1094 **Acknowledgments**

1095 We thank our many SPARK at Stanford advisors for their support, both financially and through  
1096 their invaluable advice. We wish to thank Miao Wen, Nina A. Carlos, Lawrence Huang, Cuong  
1097 Tran, Stephanie Armstrong, and Daniel Calarese of Sutro Biopharma for their help in the

1098 production of the cell-free expressed RBD, Roxanne Lopardo at Avian Vaccine Services,  
1099 Charles River Laboratories for her work in IgY testing, and David Goodkin for helpful advice  
1100 and critical review. We also thank the study staff at Linear Clinical Research Ltd and Resolutum  
1101 Global for their outstanding conduct and analysis of the phase 1 clinical study and Yael  
1102 Rosenberg-Hasson, Tyson H Holmes, Prof. Mark Davis, and other members of the Immunoassay  
1103 Team at the Human Immune Monitoring Center (Stanford University) for cytokine analyses and  
1104 statistical consultation. Linda MacKeen provided invaluable editing support.

## 1105 **References**

- 1106 1. World Health Organization. WHO Coronavirus (COVID-19) Dashboard. [Cited January 4,  
1107 2022]. Available from: <https://covid19.who.int/>
- 1108 2. University of Oxford. Vaccination by location. [Cited January 4, 2022]. Available from:  
1109 [https://ourworldindata.org/covid-vaccinations?country=OWID\\_WRL](https://ourworldindata.org/covid-vaccinations?country=OWID_WRL)
- 1110 3. Irwin A. What it will take to vaccinate the world against COVID-19. *Nature*. 2021; 592:  
1111 176-178.
- 1112 4. Lopman BA, Shioda K, Nguyen Q, Beckett SJ, Siegler AJ, Sullivan PS, et al. A framework  
1113 for monitoring population immunity to SARS-CoV-2. *Ann Epidemiol*. 2021; 63: 75-78.
- 1114 5. Koff WC, Schenkelberg T, Williams T, Baric RS, McDermott A, Cameron CM, et al.  
1115 Development and deployment of COVID-19 vaccines for those most vulnerable. *Sci*  
1116 *Transl Med*. 2021; 13: eabd1525.
- 1117 6. Pardi N, Weissman D. Development of vaccines and antivirals for combating viral  
1118 pandemics. *Nat Biomed Eng*. 2020; 4: 1128-1133.
- 1119 7. Mlcochova P, Kemp S, Dhar MS, Papa G, Meng B, Ferreira IATM., et al. SARS-CoV-2  
1120 B.1.617.2 Delta variant replication and immune evasion. *Nature*. 2021; 599: 114-119.

- 1121 8. Liu C, Ginn HM, Dejnirattisai W, Supasa P, Wang B, Tuekprakhon A, et al. Reduced  
1122 neutralization of SARS-CoV-2 B.1.617 by vaccine and convalescent serum. *Cell*. 2021;  
1123 184: 4220-4236.
- 1124 9. National Institutes of Health, National Center for Advancing Translational Sciences.  
1125 OpenData Portal. SARS-CoV-2 Variants & Therapeutics. [Cited January 4, 2022].  
1126 Available from: <https://opendata.ncats.nih.gov/variant/summary>
- 1127 10. Zhang Z, Wu S, Wu B, Yang Q, Chen A, Li Y, et al. SARS-CoV-2 Omicron strain exhibits  
1128 potent capabilities for immune evasion and viral entrance. *Sig Transduct Target Ther*.  
1129 2021; 6: 430.
- 1130 11. Cameroni E, Bowen JE, Rosen LE, Saliba C, Zepada SK, Culap K, et al. Broadly  
1131 neutralizing antibodies overcome SARS-CoV-2 Omicron antigenic shift. *Nature*.  
1132 December 23, 2021. <https://doi.org/10.1038/d41586-021-03825-4>
- 1133 12. Liu L, Iketani S, Guo Y, Chan J F-W, Wang M, Liu L, et al. Striking Antibody Evasion  
1134 Manifested by the Omicron Variant of SARS-CoV-2. *Nature*. December 23, 2021;  
1135 <https://doi.org/10.1038/d41586-021-03826-3>
- 1136 13. University of Oxford. SARS-CoV-2 variants in analyzed sequences (by country). [Cited  
1137 January 4, 2022]. Available from: [https://ourworldindata.org/grapher/covid-variants-  
1138 area?country=~USA](https://ourworldindata.org/grapher/covid-variants-area?country=~USA)
- 1139 14. Hu B, Guo H, Zhou P, Shi Z-L. Characteristics of SARS-CoV-2 and COVID-19. *Nat Rev*  
1140 *Microbiol*. 2021; 19: 141-154.
- 1141 15. Walls AC, Park Y-J, Tortorici MA, Wall A, McGuire AT, Velesler D. Structure, function,  
1142 and antigenicity of the SARS-CoV-2 spike glycoprotein. *Cell*. 2020; 181: 281-292.

- 1143 16. Zhang Z, Wu S, Wu B, Yang Q, Chen A, Li Y, et al. SARS-CoV-2 Omicron strain exhibits  
1144 potent capabilities for immune evasion and viral entrance. *Sig Transduct Target Ther.*  
1145 2021; 6: 430.
- 1146 17. Murin CD, Wilson IA, Ward AB. Antibody responses to viral infections: a structural  
1147 perspective across three different enveloped viruses. *Nat Microbiol.* 2019; 4:734–747.
- 1148 18. Weltzin R, Monath TP. Intranasal antibody prophylaxis for protection against viral disease.  
1149 *Clin Microbiol Rev.* 1999; 12: 383-393.
- 1150 19. Cai Q, Hanson JA, Steiner AR, Tran C, Masikat MR, Chen R, et al. A simplified and  
1151 robust protocol for immunoglobulin expression in *Escherichia coli* cell-free protein  
1152 synthesis systems. *Biotechnol Prog.* 2015; 31: 823-831.
- 1153 20. Zawada JF, Yin G, Steiner AR, Yang J, Naresh A, Roy SM, et al. Microscale to  
1154 manufacturing scale-up of cell-free cytokine production - a new approach for shortening  
1155 protein production development timelines. *Biotechnol Bioeng.* 2011; 108:1570-1578.
- 1156 21. SAS Institute Inc. 2015. SAS/IML<sup>®</sup> 14.1 User's Guide. Cary, NC: SAS Institute, Inc.
- 1157 22. Chan J F-W, Zhang AJ, Yuan S, Poon V K-M, Chan C C-S, Lee A C-Y, et al. Simulation  
1158 of the clinical and pathological manifestations of coronavirus disease 2019 (COVID-19) in  
1159 a Golden Syrian hamster model: implications for disease pathogenesis and transmissibility.  
1160 *Clin Infect Dis.* 2020; 71:2428-2446.
- 1161 23. Bricker TL, Darling TL, Hassan AO, Harastani HH, Soung A, Jiang X, et al. A single  
1162 intranasal or intramuscular immunization with chimpanzee adenovirus-vectored SARS-  
1163 CoV-2 vaccine protects against pneumonia in hamsters. *Cell Rep.* 2021; 20; 36:109400.

- 1164 24. Neerukonda SN, Vassell R, Herrup R, Liu S, Wang T, Takeda K, et al. Establishment of a  
1165 well-characterized SARS-CoV-2 lentiviral pseudovirus neutralization assay using 293T  
1166 cells with stable expression of ACE2 and TMPRSS2. *PLoS One*. 2021; 16: e0248348.
- 1167 25. Kollberg H, Carlander D, Olesen H, Wejåker PE, Johannesson M, Larsson A. Oral  
1168 administration of specific yolk antibodies (IgY) may prevent *Pseudomonas aeruginosa*  
1169 infections in patients with cystic fibrosis: a phase I feasibility study. *Pediatr Pulmonol*.  
1170 2003; 35:433-440.
- 1171 26. Lee C-D, Sun H-C, Hu S-M, Chiu C-F, Homhuan A, Liang S-M, et al. An improved  
1172 SUMO fusion protein system for effective production of native proteins. *Protein Sci*. 2008;  
1173 17: 1241-1248.
- 1174 27. Pokhrel S, Kraemer BR, Lee L, Samardzic K, Mochly-Rosen D. Increased elastase  
1175 sensitivity and decreased intramolecular interactions in the more transmissible 501Y.V1  
1176 and 501Y.V2 SARS-CoV-2 variants' spike protein-an in silico analysis. *PLoS One*. 2021;  
1177 16: e0251426.
- 1178 28. Pokhrel S, Kraemer BR, Burkholz S, Mochly-Rosen D. Natural variants in SARS-CoV-2  
1179 Spike protein pinpoint structural and functional hotspots with implications for prophylaxis  
1180 and therapeutic strategies. *Sci Rep*. 2021; 11: 13120.
- 1181 29. (no authors) COVID-19 Vaccine Comparison Chart. *Med Lett Drug Ther*. [Cited January  
1182 4, 2022]. Available from: [https://secure.medicalletter.org/downloads/1621g\\_table.pdf](https://secure.medicalletter.org/downloads/1621g_table.pdf)
- 1183 30. Dejnirattisai W, Shaw RH, Supasa P, Liu C, Stuart AS, Pollard AJ, et al. Reduced  
1184 neutralisation of SARS-CoV-2 omicron B.1.1.529 variant by post-immunisation serum  
1185 *Lancet*. 2021; S0140-6736:02844-0.

- 1186 31. Chemical Computing Group. Molecular Operating Environment (MOE). Montreal,  
1187 Canada. 2021.
- 1188 32. Centers for Disease Control and Prevention. Science Brief: Omicron (B.1.1.529) variant.  
1189 [Cited January 4, 2022]. Available from: [https://www.cdc.gov/coronavirus/2019-](https://www.cdc.gov/coronavirus/2019-ncov/science/science-briefs/scientific-brief-omicron-variant.html)  
1190 [ncov/science/science-briefs/scientific-brief-omicron-variant.html](https://www.cdc.gov/coronavirus/2019-ncov/science/science-briefs/scientific-brief-omicron-variant.html)
- 1191 33. Centers for Disease Control and Prevention. Potential Rapid Increase of Omicron Variant  
1192 Infections in the United States. [Cited January 4, 2022]. Available from:  
1193 [https://www.cdc.gov/coronavirus/2019-ncov/science/forecasting/mathematical-modeling-](https://www.cdc.gov/coronavirus/2019-ncov/science/forecasting/mathematical-modeling-outbreak.html)  
1194 [outbreak.html](https://www.cdc.gov/coronavirus/2019-ncov/science/forecasting/mathematical-modeling-outbreak.html)
- 1195 34. Carlander D, Stålberg J, Larsson A. Chicken antibodies: a clinical chemistry perspective.  
1196 Ups J Med Sci. 1999; 104:179-189.
- 1197 35. Lee L, Samardzic K, Wallach M, Frumkin LR, Mochly-Rosen D. Immunoglobulin Y for  
1198 potential diagnostic and therapeutic applications in infectious diseases. Front Immunol.  
1199 2021;12:696003.
- 1200 36. Artman C, Brumfield KD, Khanna S, Goepp J. Avian antibodies (IgY) targeting spike  
1201 glycoprotein of severe acute respiratory syndrome coronavirus 2 (SARS-CoV-2) inhibit  
1202 receptor binding and viral replication. PLoS One. 2021;16:e0252399.
- 1203 37. Shen H, Cai Y, Zhang H, Wu J, Ye L, Yang P, et al. Anti-SARS-CoV-2 IgY isolated from  
1204 egg yolks of hens immunized with inactivated SARS-CoV-2 for immunoprophylaxis of  
1205 COVID-19. Virol Sin. 2021; 36:1080-1082.
- 1206 38. Bao L, Zhang C, Lyu J, Yi P, Shen X, Tang B, et al. Egg yolk immunoglobulin (IgY)  
1207 targeting SARS-CoV-2 S1 as potential virus entry blocker. J Appl Microbiol. 2021 Oct  
1208 27:10.1111/jam.15340. doi: 10.1111/jam.15340.

- 1209 39. Wei S, Duan S, Liu X, Wang H, Ding S, Chen Y, et al. Chicken egg yolk antibodies (IgYs)  
1210 block the binding of multiple SARS-CoV-2 spike protein variants to human ACE2. *Int*  
1211 *Immunopharmacol.* 2021;90:107172.
- 1212 40. Lu Y, Wang Y, Zhang Z, Huang J, Yao M, Huang G, et al. Generation of chicken IgY  
1213 against SARS-COV-2 spike protein and epitope mapping. *J Immunol Res.*  
1214 2020;2020:9465398.
- 1215 41. Lyu J, Bao L, Shen X, Yan C, Zhang C, Wei W, et al. The preparation of N-IgY targeting  
1216 SARS-CoV-2 and its immunomodulation to IFN- $\gamma$  production in vitro. *Int*  
1217 *Immunopharmacol.* 2021;96:107797.
- 1218 42. Martin E, Schipper GM, Verhoef JC, Merkus WHM. Nasal mucociliary clearance as a  
1219 factor in nasal drug delivery. *Adv Drug Deliv Rev.* 1998; 29: 13-38.
- 1220 43. Keller MA, Stiehm ER. Passive immunity in prevention and treatment of infectious  
1221 diseases. *Clin Microbiol Rev.* 2000; 13: 602-614.
- 1222 44. Hemmingsson P, Hammarström L. Nasal administration of immunoglobulin as effective  
1223 prophylaxis against infections in elite cross-country skiers. *Scand J Infect Dis.* 1993; 25:  
1224 783-785.
- 1225 45. Lindberg K, Berglund B. Effect of treatment with nasal IgA on the incidence of infectious  
1226 disease in world-class canoeists. *Int J Sports Med.* 1996; 17: 235-238.
- 1227 46. Giraudi V, Riganti C, Torales MR, Sédola H, Gaddi E. Upper respiratory infections in  
1228 children: Response to endonasal administration of IGA. *Int J Pediatr Otorhinolaryngol.*  
1229 1997; 39: 103-110.



- 1230 47. Heikkinen TA, Ruohola A, Ruuskanen O, Waris M, Uhari M, Hammarström L.  
1231 Intranasally administered immunoglobulin for the prevention of rhinitis in children. *Pediatr*  
1232 *Infect Dis J.* 1998; 17: 367-372.
- 1233 48. Gleich GJ, Yunginger JW. Ragweed hay fever: treatment by local passive administration  
1234 of IgG antibody. *Clin Allergy.* 1975; 5:79-87.
- 1235 49. Hou YJ, Okuda K, Edwards CE, Martinez DR, Asakura T, Dinnon KH 3rd, et al. SARS-  
1236 CoV-2 Reverse genetics reveals a variable infection gradient in the respiratory tract. *Cell.*  
1237 2020; 182: 429-446.e14.
- 1238 50. Mason RJ. Pathogenesis of COVID-19 from a cell biology perspective. *Eur Respiratory J.*  
1239 2020; 55: 2000607.
- 1240 51. Kovacs-Nolan J, Mine Y. Egg yolk antibodies for passive immunity. *Ann Rev Food Sci*  
1241 *Technol.* 2012; 3: 163-182.
- 1242 52. Kim Y-II, Kim D, Yu K-M, Seo HD, Lee S-A, Casel MAB, et al. Development of Spike  
1243 receptor-binding domain nanoparticles as a vaccine candidate against SARS-CoV-2  
1244 infection in ferrets. *mBio.* 2021; 12: e00230-21.
- 1245 53. Palit P, Chattopadhyay D, Thomas SS, Kundu A, Kim HS, Rezaeif N.  
1246 Phytopharmaceuticals mediated Furin and TMPRSS2 receptor blocking: can it be a  
1247 potential therapeutic option for Covid-19? *Phytomedicine.* 2021; 85: 153396.
- 1248 54. Burton MJ, Clarkson JE, Goulao B, Glenney A-M, McBain AJ, Schilder AG, et al.  
1249 Worthington, Use of antimicrobial mouthwashes (gargling) and nasal sprays by healthcare  
1250 workers to protect them when treating patients with suspected or confirmed COVID-19  
1251 infection. *Cochrane Database Syst Rev.* 2021; 9: CD013626.

- 1252 55. Higgins TS, Wu AW, Illing EA, Sokoloski KJ, Weaver BA, Anthony BP, et al. Intranasal  
1253 antiviral drug delivery and coronavirus disease 2019 (COVID-19): A state of the art  
1254 review. *Otolaryngol Head Neck Surg.* 2021; 163:682-694.
- 1255 56. Ku Z, Xie X, Hinton PR, Liu X, Ye X, Muruato AE, et al. Nasal delivery of an IgM offers  
1256 broad protection from SARS-CoV-2 variants. *Nature.* 2021; 595: 718-723.
- 1257 57. Nambulli S, Xiang Y, Tilston-Lunel NL, Rennick LJ, Sang Z, Klimstra WB, et al.  
1258 Inhalable nanobody (PiN-21) prevents and treats SARS-CoV-2 infections in Syrian  
1259 hamsters at ultra-low doses. *Sci Adv.* 2021; 7: eabh0319.
- 1260 58. Fu Y, Maruyama J, Singh A, Lim R, Ledesma A, Lee D, et al. Protective effects of sti-  
1261 2020 antibody delivered post-infection by the intranasal or intravenous route in a Syrian  
1262 Golden Hamster COVID-19 model. *bioRxiv [Preprint]*. Posted October 29, 2020, Cited  
1263 January 4, 2022. Available from:  
1264 <https://www.biorxiv.org/content/10.1101/2020.10.28.359836v1>
- 1265 59. Watanabe Y, Berndsen ZT, Raghvani J, Seabright GE, Allen JD, Pybus OG, et al.  
1266 Vulnerabilities in coronavirus glycan shields despite extensive glycosylation. *Nat*  
1267 *Commun.* 2020; 11: 2688.
- 1268 60. Fournillier A, Wychowski C, Boucreux D, Baumert TF, Meunier JC, Jacobs D, et al.  
1269 Induction of hepatitis C virus E1 envelope protein-specific immune response can be  
1270 enhanced by mutation of N-glycosylation sites. *J Virol.* 2001; 75:12088-12097.
- 1271 61. Schade R, Gutierrez Calzado E, Sarmiento R, Chacana PA, Porankiewicz-Asplund J,  
1272 Terzolo HR. Chicken egg yolk antibodies (IgY-technology): a review of progress in

1273 production and use in research and human and veterinary medicine. *Altern Lab Anim.*  
1274 2005; 33:129-154.

1275

## 1276 **Supporting information captions**

1277 **S1 Protocol. Phase 1 Clinical Trial Protocol.**

1278 **S1 CONSORT Checklist.**

1279 **S1 Table. Rat toxicity study protocol.**

1280 **S2 Table. Bioanalytical sample collection from the rat toxicity study.**

1281 **S3 Table. Cytokine sample collection for the rat toxicity study.**

1282 **S4 Table. Human tissue cross-reactivity; list of tissues examined.**

1283 **S1 Figure. Efficacy study in hamsters.** Placebo control and IgY-treated Syrian hamsters were  
1284 challenged with  $4 \times 10^6$  or  $8 \times 10^5$  PFU SARS-CoV-2; titer was determined in Vero E6 cells.  
1285 However, the viral titers on Vero-hACE2-hTMPRSS2, which includes the essential protease to  
1286 liberate the RBD from the S protein on the surface of the virus [24], was almost 100-fold higher  
1287 at  $4 \times 10^6$  or  $0.8 \times 10^6$ . Infectious virus titers were measured in the lungs 3 days post-infection by  
1288 plaque assay. Each symbol is a single animal. One animal in the placebo group challenged with a  
1289 low dose of the virus did not have any detectable virus in the lung homogenate. This was ruled  
1290 an outlier based on the viral RNA levels in other assays. Viral RNA levels were assessed by RT-  
1291 qPCR in lung homogenates of nasal swabs using 2 different primer-probe sets. Each symbol is a  
1292 single animal and the bars represent the geometric mean with geometric standard deviation.

1293 **S2 Figure. Serum cytokines from study participants.** Serum cytokines for human participants  
1294 in the phase 1 study. Blood cytokine levels before treatment (D1 pre-dose), 2 hours after the first  
1295 treatment (D1H2), 24 hours after 3-times daily intranasal (D2 pre-dose), and 2 hours after the

1296 first dose on the second day (D2H2) of anti-SARS-CoV-2 RBD IgY (0, 2, 4 and 8 mg/dose).  
1297 Data are adjusted for nonspecific binding and plate artifacts plus the effects of individual  
1298 persons. Red indicates a statistical difference with a false discovery rate (FDR) significant p-  
1299 value ( $p < 0.05$ ).

### 1300 **Funding**

1301 This project was supported by funds from SPARK at Stanford, SPARK GLOBAL, and grants  
1302 from the Booz-Allen Foundation and ChEM-H (Stanford University). We are also grateful for  
1303 the financial support from the Moonchu Foundation, the Human Immune Monitoring Center  
1304 (HIMC) at Stanford University, and the generous monetary donations of many others. The  
1305 funders had no role in study design, data collection and analysis, decision to publish, or  
1306 preparation of the manuscript.

### 1307 **Competing interests**

1308 None of the authors declare competing interests.

### 1309 **Data and materials availability**

1310 All data are available in the main text or Supporting Information. The study is registered at  
1311 ClinicalTrials.gov (<https://clinicaltrials.gov/ct2/show/NCT04567810>).

1312

### 1313 **Disclaimer**

1314 Opinions, conclusions, interpretations, and recommendations are those of the authors and are not  
1315 necessarily endorsed by the U.S. Army. The mention of trade names or commercial products  
1316 does not constitute endorsement or recommendation for use by the Department of the Army or  
1317 the Department of Defense.

1318

1319 **Author contributions**

1320 **Conceptualization:** Michael Wallach, Daria Mochly-Rosen, Lyn R. Frumkin

1321 **Methodology:** Lyn R. Frumkin, Michaela Lucas, Curtis L. Scribner, Nastassja Ortega-Heinly,

1322 Alice Yam, Trevor J Hallam, Alice Yam, Kristin Bedard, Courtney A. Cohen, John M. Dye,

1323 Brian McMillan, Adrianus C.M. Boon, Tom St. John

1324 **Investigation:** Michaela Lucas, Nastassja Ortega-Heinly, Gang Yin, Courtney A. Cohen,

1325 Catherine V. Badger, Shawn A. Abbasi, Traci L. Bricker, Astha Joshi, Suman Pokhrel, Benjamin

1326 R. Kraemer, Lucia Lee

1327 **Visualization:** Lucia Lee, Daria Mochly-Rosen

1328 **Funding Acquisition:** Daria Mochly-Rosen, Stephen Kargotich

1329 **Project Administration:** Mahima Agogiya, Rebecca Begley, Lucia Lee, Jayden Rogers

1330 **Supervision:** Jayden Rogers, John M. Dye, Brian McMillan, Trevor J Hallam, Adrianus C.M.

1331 Boon, Stephen Kargotich, Daria Mochly-Rosen

1332 **Writing – original draft:** Daria Mochly-Rosen, Lyn R. Frumkin

1333 **Writing – review - all authors**

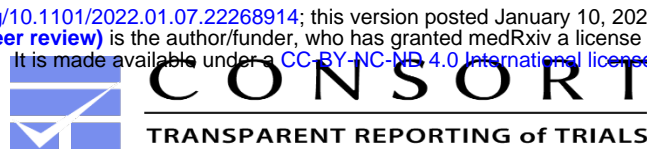
1334 **Writing – editing:** Daria Mochly-Rosen, Lyn R. Frumkin, Benjamin R. Kraemer, Tom St. John

1335

1336

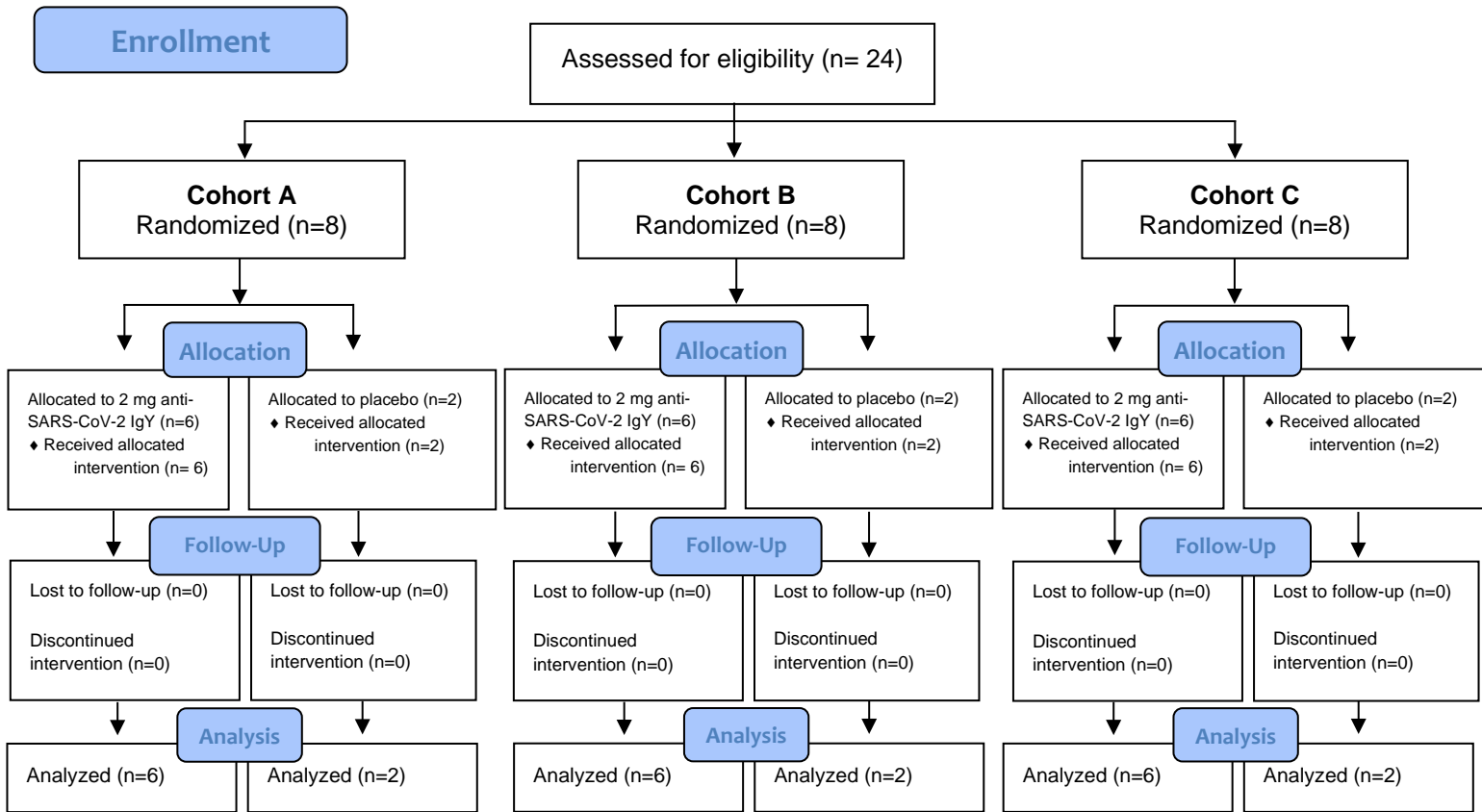
1337

FIG 1



## CONSORT 2010 Flow Diagram

### Part I: Single-Ascending Dose (Cohorts A-C consecutively enrolled)



### Part II: Multiple Dose (concurrent enrollment)

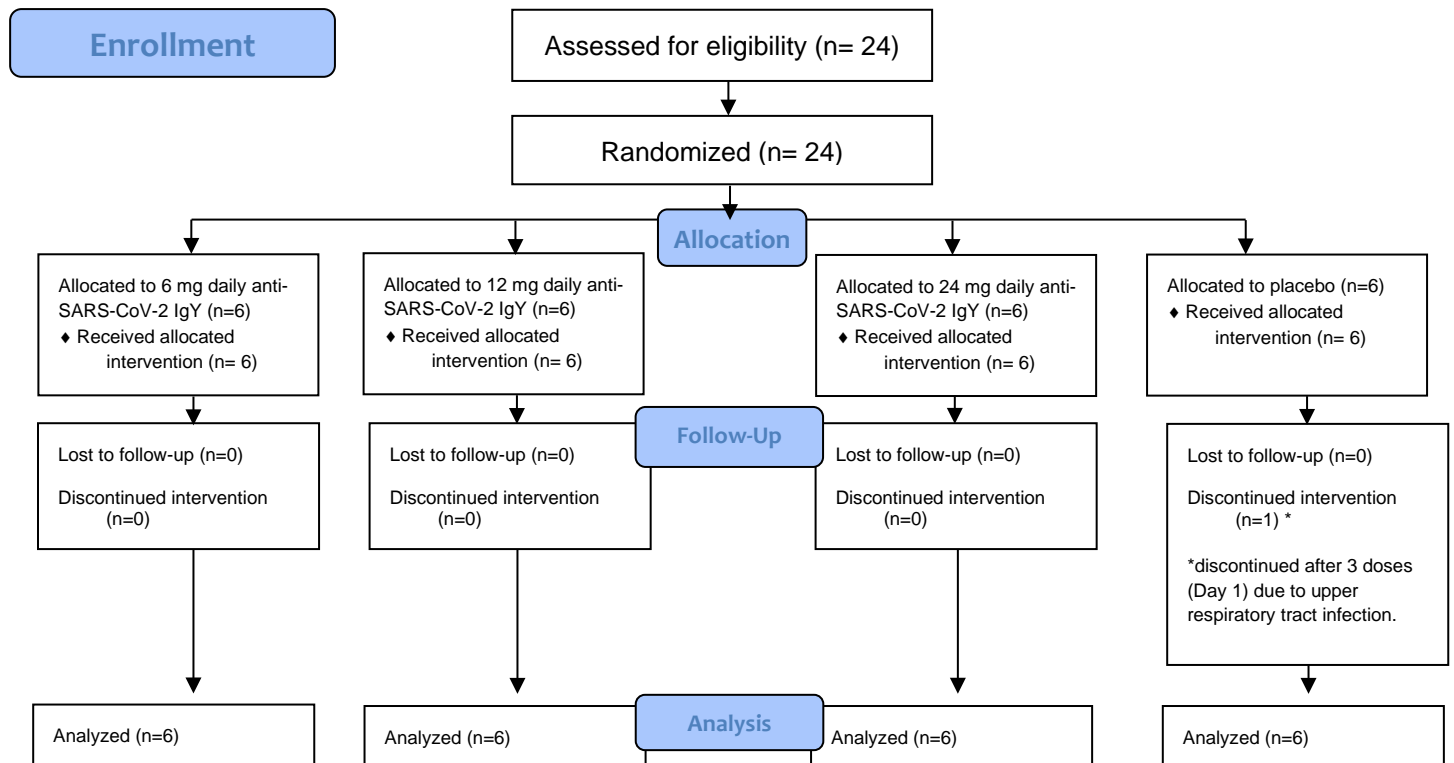


**FIG 2**

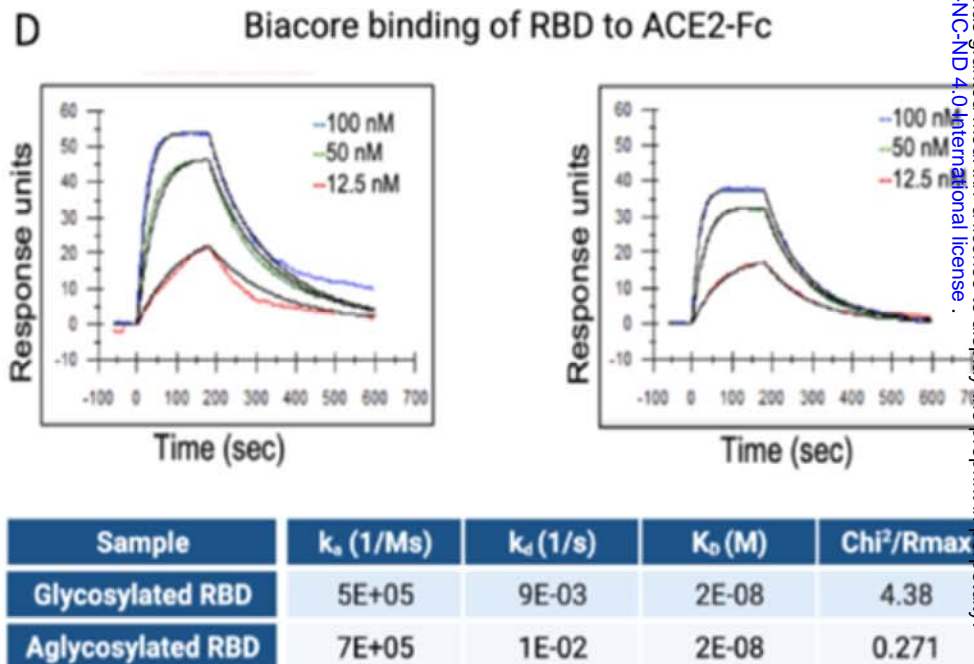
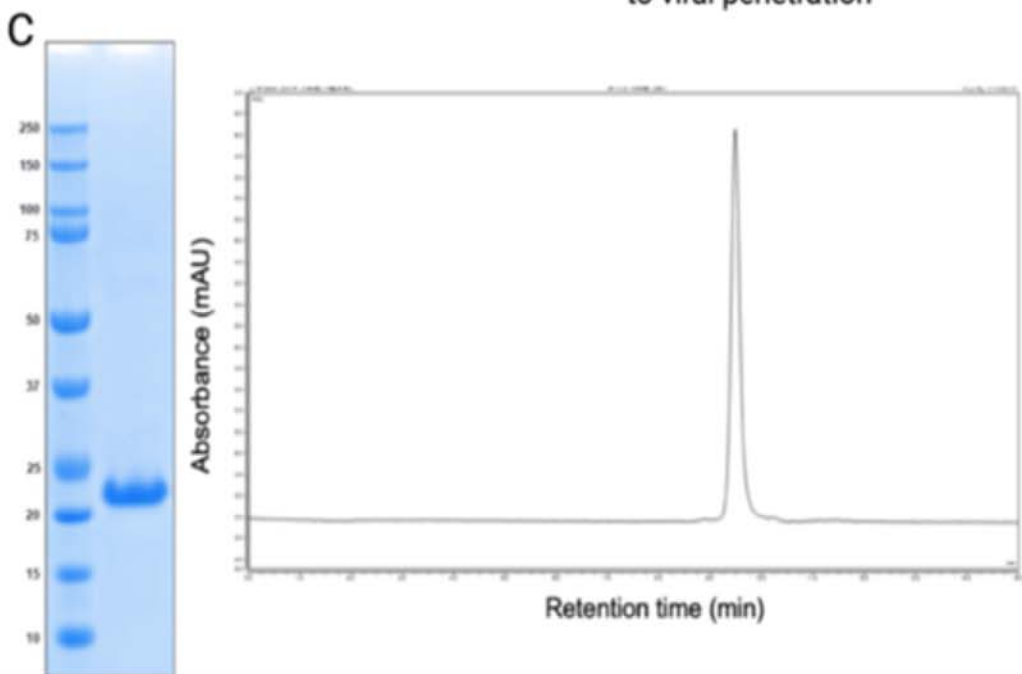
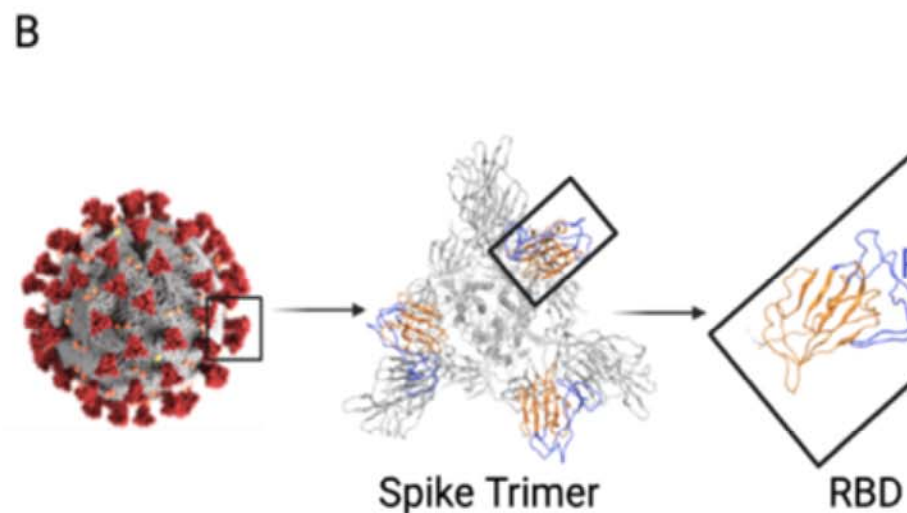
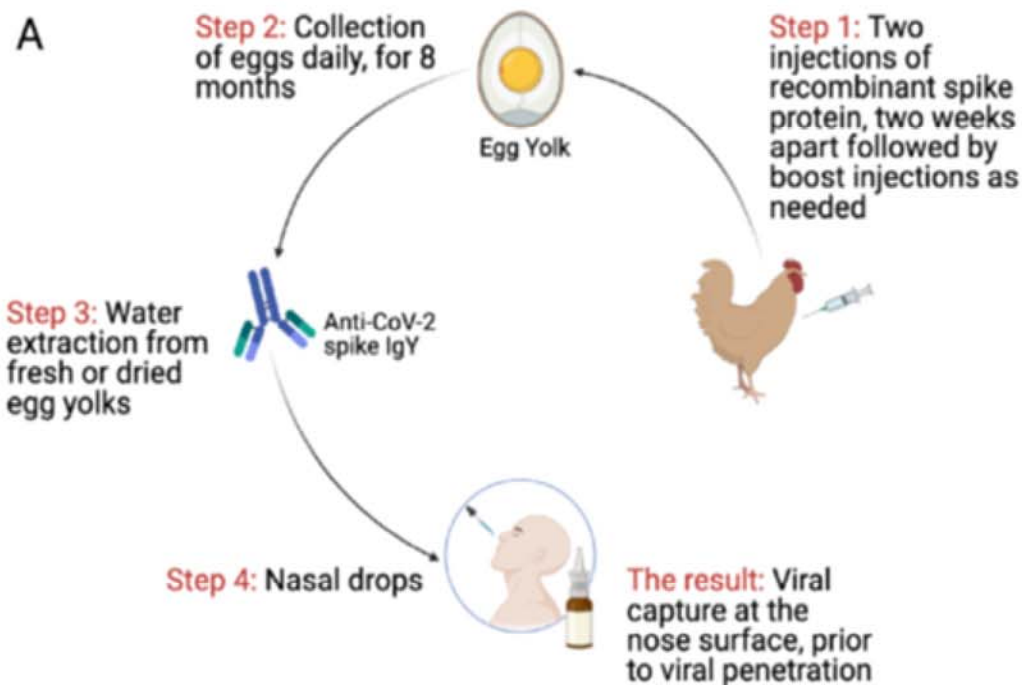


**Fig 3**

**FIG 3**

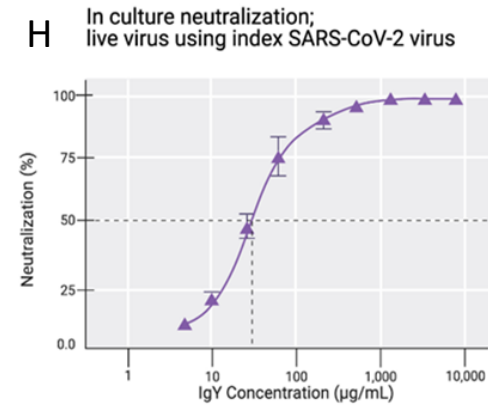
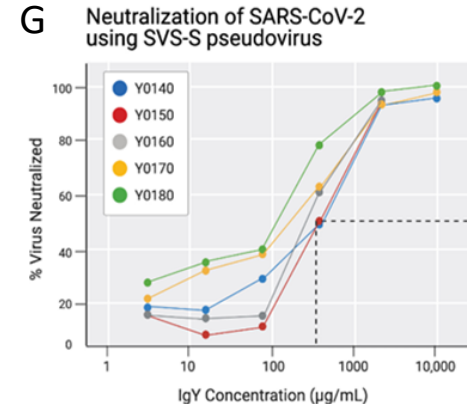
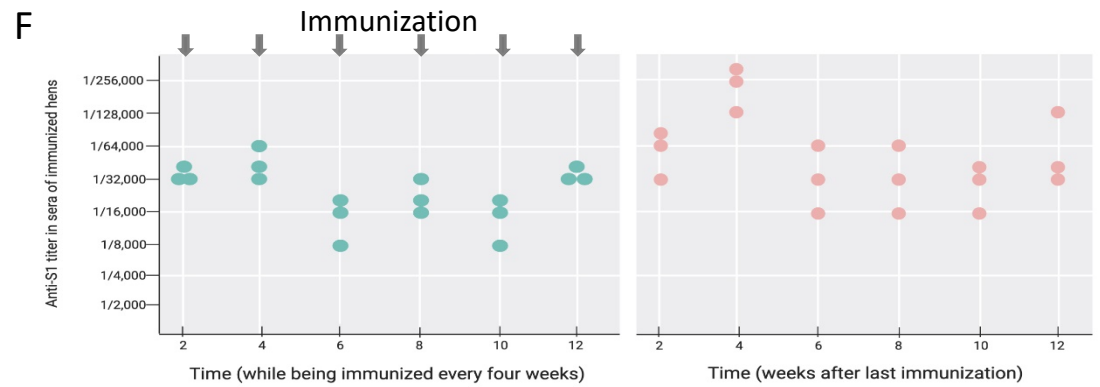
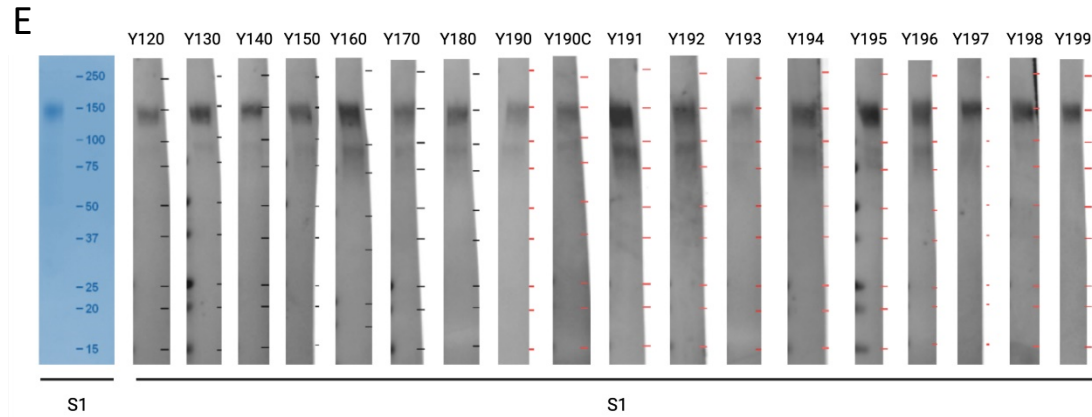
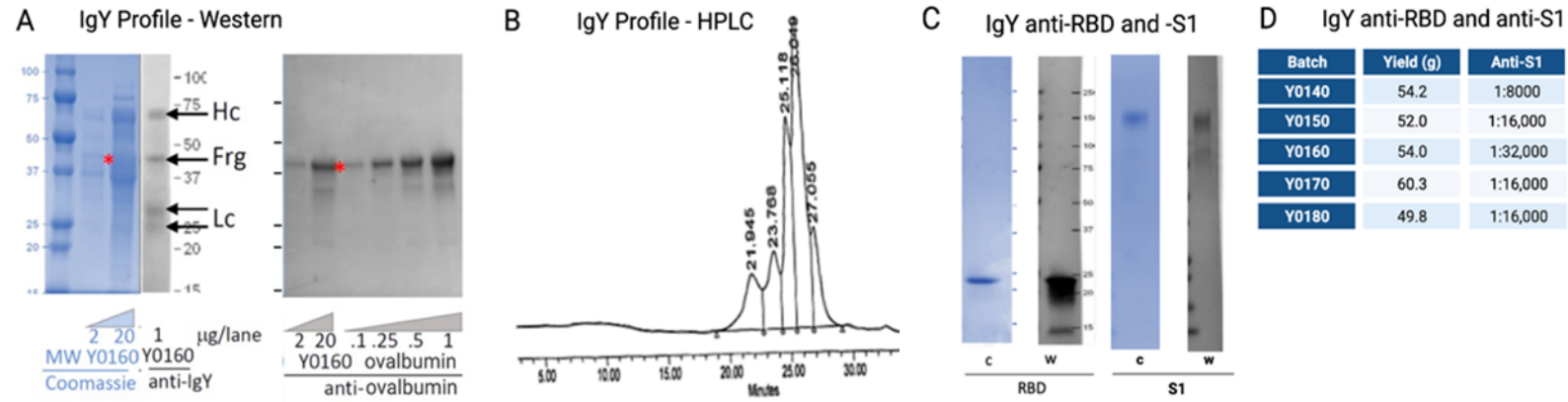
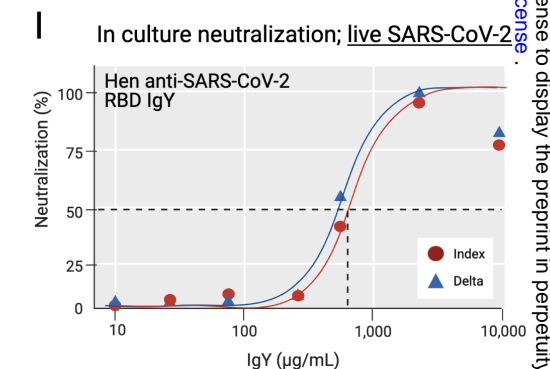
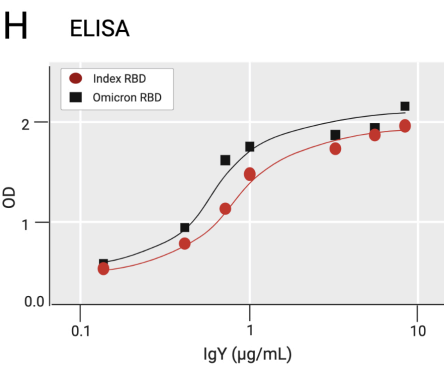
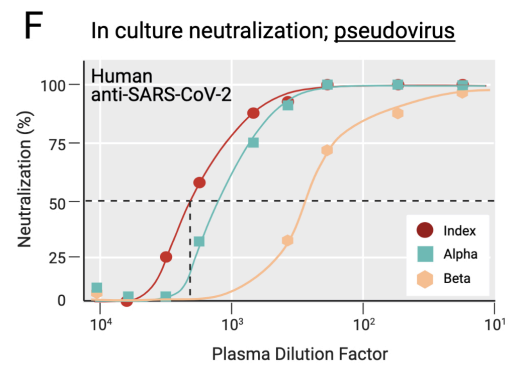
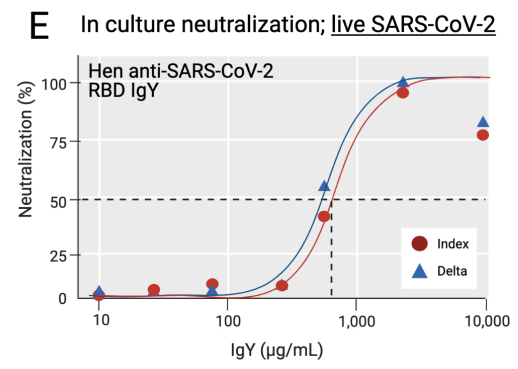
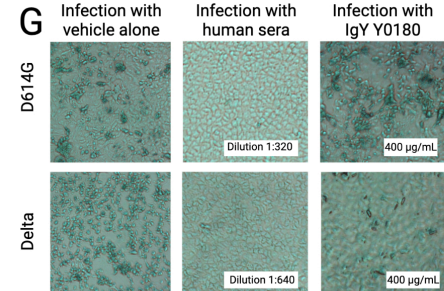
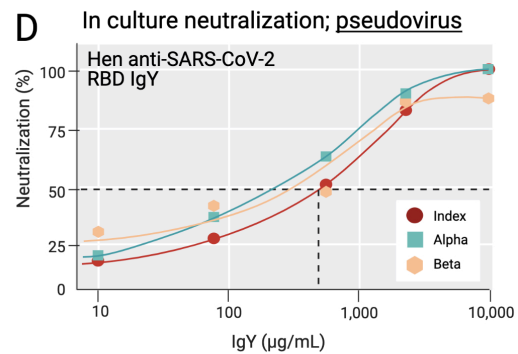
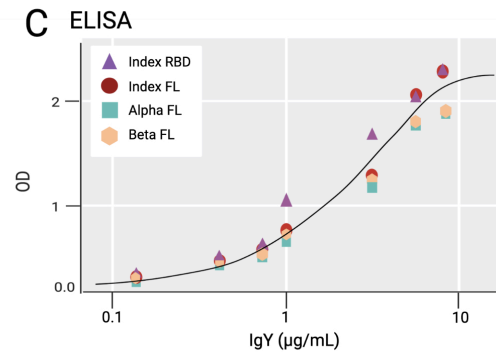
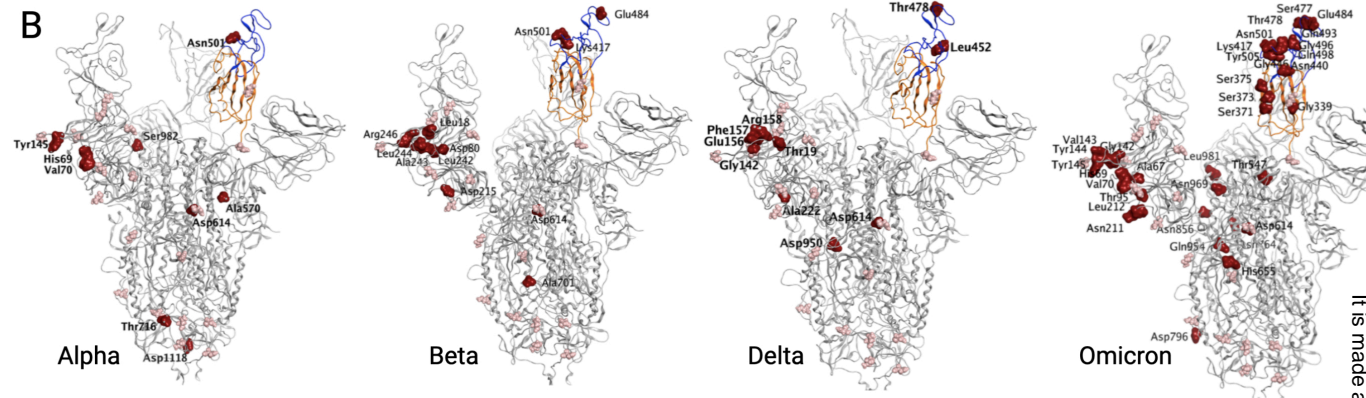
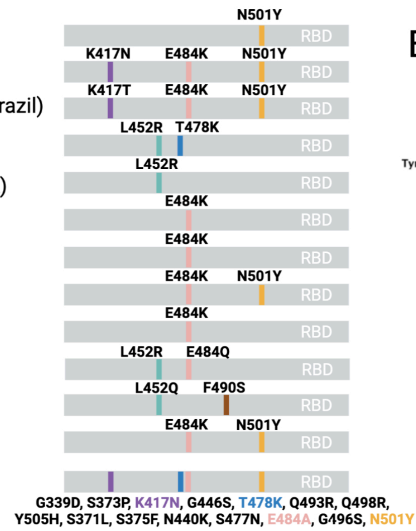




**FIG 4**

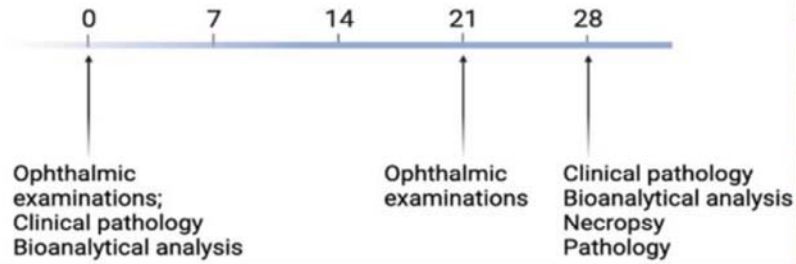
**A** Alpha/B.1.1.7 (UK)  
 Beta/B.1.351 (SA)  
 Gamma/P.1 B.1.1.248 (Brazil)  
 Delta/B.1.617.2 (India)  
 Epsilon/B.1.427/429 (CA)  
 Zeta/P.2 (Brazil)  
 Eta/B.1.525 (UK)  
 Theta/P.3 (Philippines)  
 Iota/B.1.526 (NY)  
 Kappa/B.1.617.1 (India)  
 Lambda/C.37 (Peru)  
 Mu/B.1.621 (Colombia)  
 Omicron/B.1.1529 (SA)



medRxiv preprint doi: <https://doi.org/10.1101/2022.01.07.22268914>; this version posted January 10, 2022. The copyright holder for this preprint (which was not certified by peer review) is the author/funder, who has granted medRxiv a license to display the preprint in perpetuity. It is made available under a [CC-BY-NC-ND 4.0 International license](#).

FIG 5

**A** Twice daily treatment @ 4 mg or vehicle  
(0 or 1mg/nare/dose)



**B**

TEST	FINDINGS
CLINICAL OBSERVATIONS	No drug-related clinical observations.
CLINICAL PATHOLOGY	No differences in hematology, coagulation, or clinical chemistry parameters.
FOOD CONSUMPTION	No notable differences in food consumption.
BODY WEIGHT	No notable differences in mean body weights.
OPHTHALMIC	No drug-related ocular findings
NECROPSY OBSERVATIONS	No drug-related macroscopic and microscopic findings, including nasal histology.

**C**

D1H0 is Common Comparator Timepoint within a Treatment  
Red Denotes FDR Significant p-value ( $p < 0.05$ ).

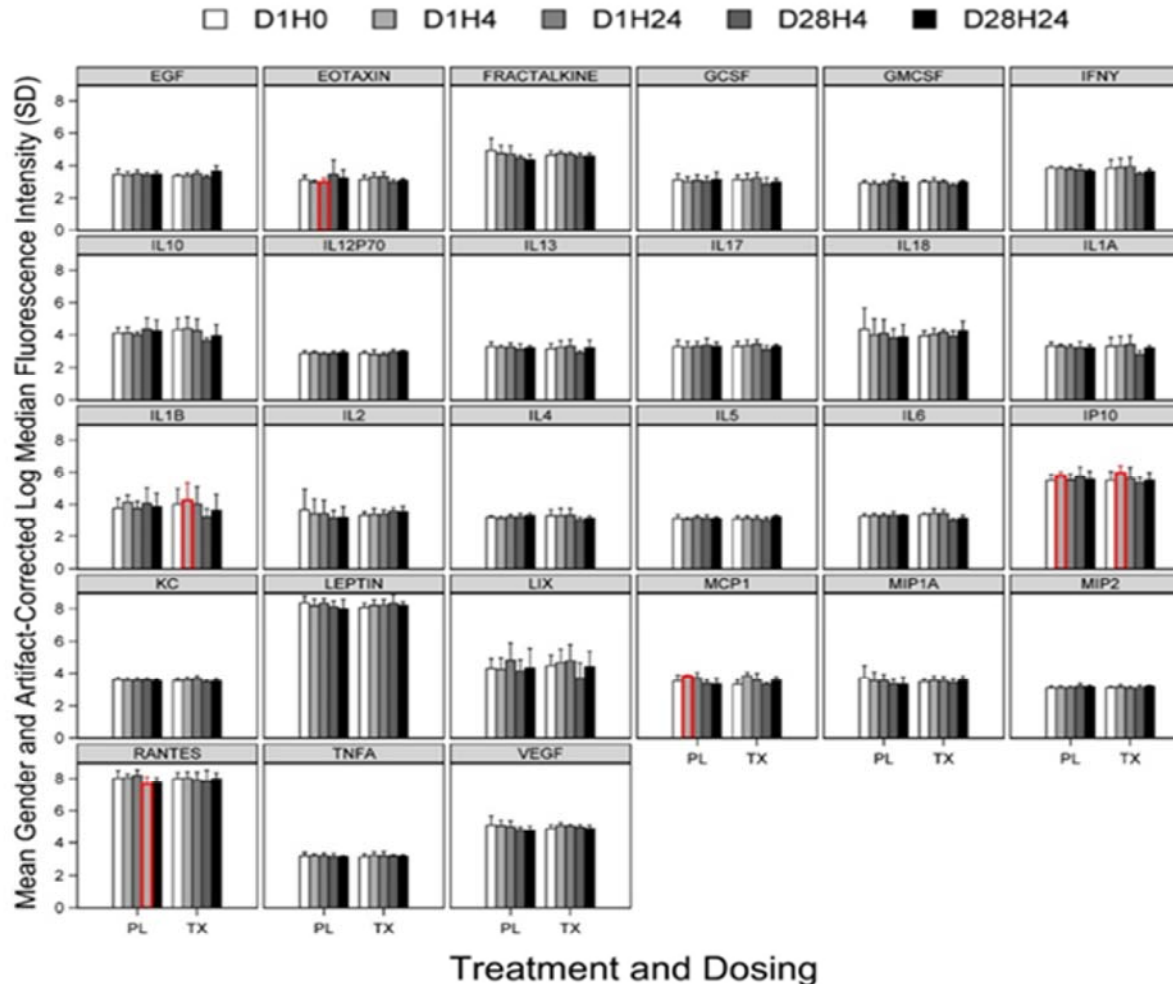
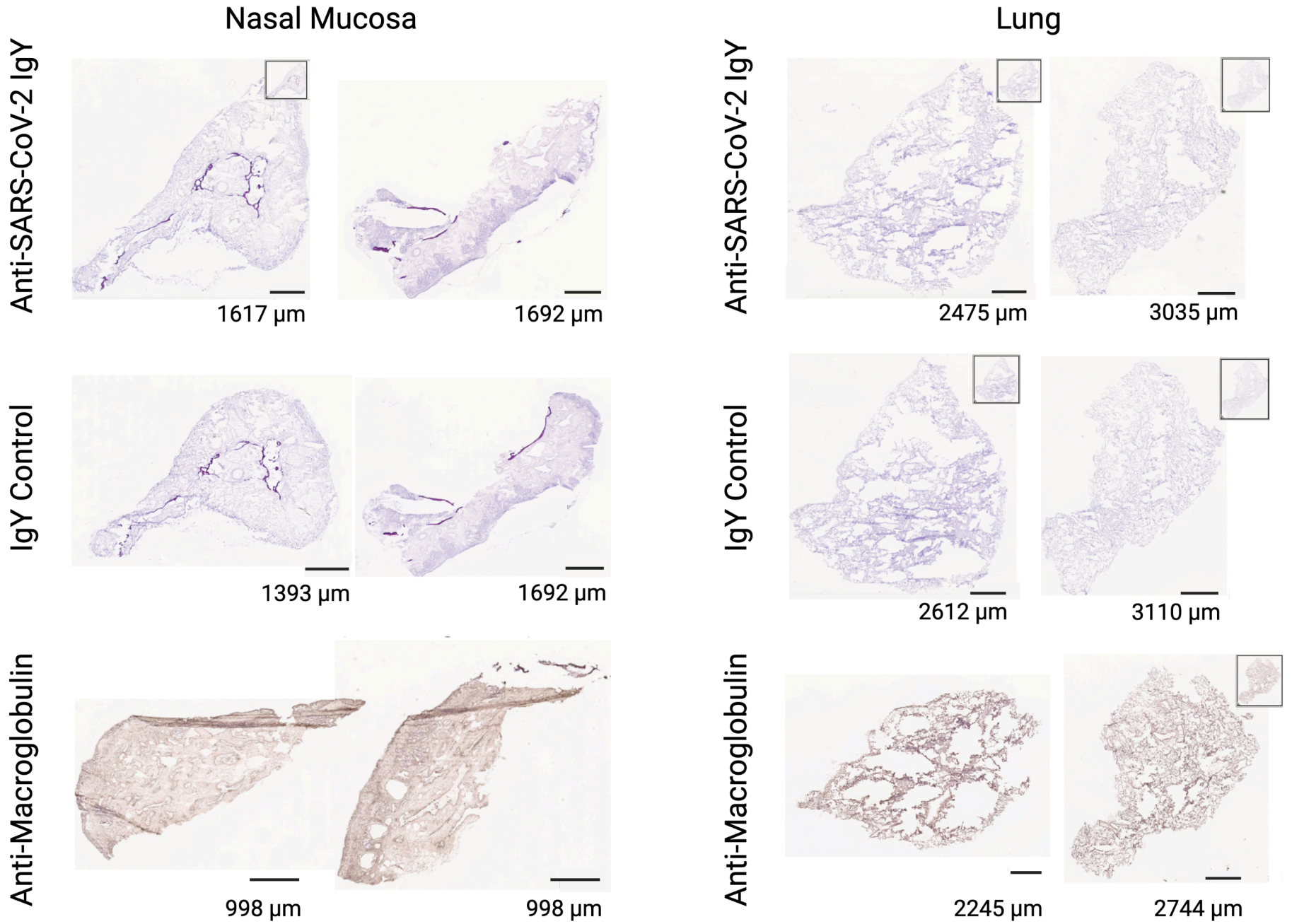


**FIG 6**



## S1 Protocol



**Protocol Number: CVR001**

**A Phase 1 Study in Healthy Participants to Evaluate the Safety,  
Tolerability, and Pharmacokinetics of Single-Ascending and  
Multiple Doses of an Anti-Severe Acute Respiratory Syndrome  
Coronavirus 2 (SARS-CoV-2) Chicken Egg Antibody (IgY)**

**Investigational Drug: Anti-SARS-CoV-2 IgY**

Sponsor:  
SPARK at Stanford

Sponsor Contact:  
Daria Mochly-Rosen, PhD  
Professor, Dept. of Chemical and Systems Biology  
George D. Smith Professor of Translational Medicine  
CCSR Room 3145a, 269 Campus Drive  
Stanford University School of Medicine  
Stanford, California 94305-5174  
Tel: (650) 725-7720 (mobile)  
E-mail: [mochly@stanford.edu](mailto:mochly@stanford.edu)

**Version 3.0, dated 29 September 2020**

The information contained in this protocol is confidential and intended for the use of the study staff. The information in this document is the property of the sponsor and may not be disclosed unless federal or state law or regulations require such disclosure. Subject to the foregoing, this information may be disclosed only to those persons involved in the study who need to know, with the obligation not to further disseminate this information.

# S1 CONSORT Checklist



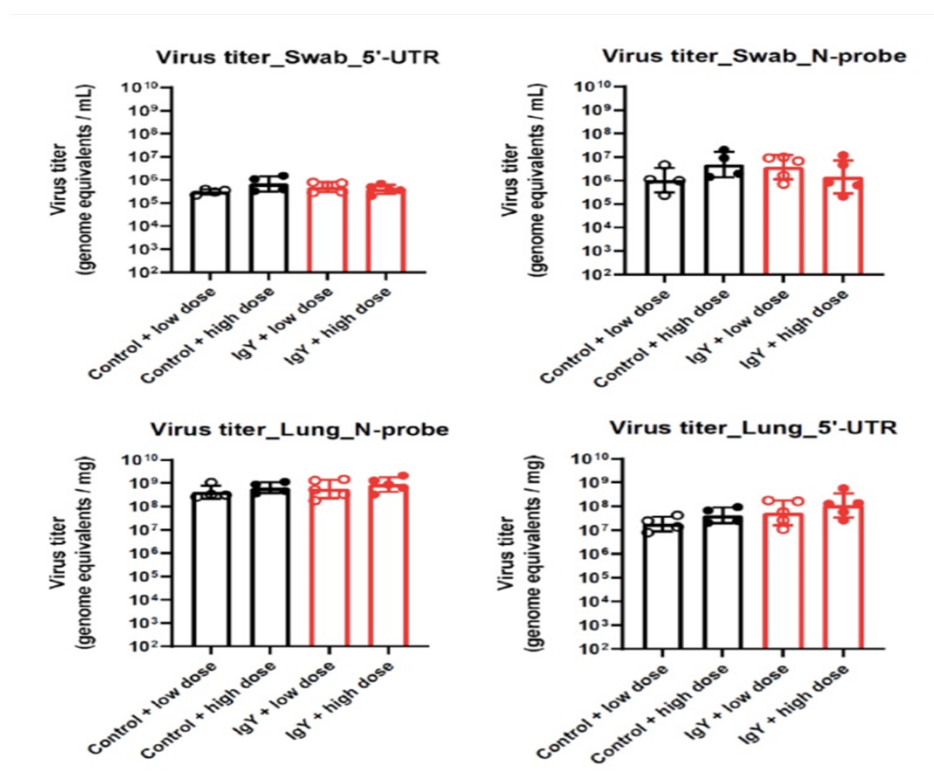
## CONSORT 2010 checklist of information to include when reporting a randomised trial\*

Section/Topic	Item No	Checklist item	Reported on page No
<b>Title and abstract</b>			
	1a	Identification as a randomised trial in the title	1
	1b	Structured summary of trial design, methods, results, and conclusions (for specific guidance see CONSORT for abstracts)	3
<b>Introduction</b>			
Background and objectives	2a	Scientific background and explanation of rationale	4-7
	2b	Specific objectives or hypotheses	6-7
<b>Methods</b>			
Trial design	3a	Description of trial design (such as parallel, factorial) including allocation ratio	11-18
	3b	Important changes to methods after trial commencement (such as eligibility criteria), with reasons	NA
Participants	4a	Eligibility criteria for participants	11
	4b	Settings and locations where the data were collected	11
Interventions	5	The interventions for each group with sufficient details to allow replication, including how and when they were actually administered	11-18
Outcomes	6a	Completely defined pre-specified primary and secondary outcome measures, including how and when they were assessed	11-18
	6b	Any changes to trial outcomes after the trial commenced, with reasons	NA
Sample size	7a	How sample size was determined	16
	7b	When applicable, explanation of any interim analyses and stopping guidelines	16-17
<b>Randomisation:</b>			
Sequence generation	8a	Method used to generate the random allocation sequence	11-12
	8b	Type of randomisation; details of any restriction (such as blocking and block size)	11-12
Allocation concealment mechanism	9	Mechanism used to implement the random allocation sequence (such as sequentially numbered containers), describing any steps taken to conceal the sequence until interventions were assigned	11-12
Implementation	10	Who generated the random allocation sequence, who enrolled participants, and who assigned participants to interventions	11-12
Blinding	11a	If done, who was blinded after assignment to interventions (for example, participants, care providers, those	11

		assessing outcomes) and how	
	11b	If relevant, description of the similarity of interventions	NA
Statistical methods	12a	Statistical methods used to compare groups for primary and secondary outcomes	16
	12b	Methods for additional analyses, such as subgroup analyses and adjusted analyses	NA
<b>Results</b>			
Participant flow (a diagram is strongly recommended)	13a	For each group, the numbers of participants who were randomly assigned, received intended treatment, and were analysed for the primary outcome	11
	13b	For each group, losses and exclusions after randomisation, together with reasons	38
Recruitment	14a	Dates defining the periods of recruitment and follow-up	11
	14b	Why the trial ended or was stopped	NA
Baseline data	15	A table showing baseline demographic and clinical characteristics for each group	26-27
Numbers analysed	16	For each group, number of participants (denominator) included in each analysis and whether the analysis was by original assigned groups	11-18
Outcomes and estimation	17a	For each primary and secondary outcome, results for each group, and the estimated effect size and its precision (such as 95% confidence interval)	27-29
	17b	For binary outcomes, presentation of both absolute and relative effect sizes is recommended	27-29
Ancillary analyses	18	Results of any other analyses performed, including subgroup analyses and adjusted analyses, distinguishing pre-specified from exploratory	30
Harms	19	All important harms or unintended effects in each group (for specific guidance see CONSORT for harms)	27-28
<b>Discussion</b>			
Limitations	20	Trial limitations, addressing sources of potential bias, imprecision, and, if relevant, multiplicity of analyses	30
Generalisability	21	Generalisability (external validity, applicability) of the trial findings	30
Interpretation	22	Interpretation consistent with results, balancing benefits and harms, and considering other relevant evidence	30-37
<b>Other information</b>			
Registration	23	Registration number and name of trial registry	11
Protocol	24	Where the full trial protocol can be accessed, if available	S2 Supporting Information
Funding	25	Sources of funding and other support (such as supply of drugs), role of funders	49

\*We strongly recommend reading this statement in conjunction with the CONSORT 2010 Explanation and Elaboration for important clarifications on all the items. If relevant, we also recommend reading CONSORT extensions for cluster randomised trials, non-inferiority and equivalence trials, non-pharmacological treatments, herbal interventions, and pragmatic trials. Additional extensions are forthcoming: for those and for up to date references relevant to this checklist, see [www.consort-statement.org](http://www.consort-statement.org).

## S1 Fig







**S1 Table. The experimental protocol of rat toxicity study**

Group No.	Test Material	Dose Volume ( $\mu$ L dose)	Dose Concentration (mg/mL)	No. of Animals			
				Main Study		Toxicokinetic Study	
				Males	Females	Males	Females
1	Control Article	100	0	10	10	3	3
2	IgY SARS-CoV-2 RBD	100	20	10	10	6	6
3	Control Article	100	0	3 <sup>a</sup>	3 <sup>a</sup>	-	-
4	IgY SARS-CoV-2 RBD	100	20	3 <sup>a</sup>	3 <sup>a</sup>	-	-

<sup>a</sup> = These animals were for cytokine analysis only.

**S2 Table. Bioanalytical sample collection from the rat toxicity study**

Group No.	Subgroup	No. of Animals (M/F)	(Time Post the first daily dose) on Day 1		
			15 min	6 <sup>a</sup> hr	24 hr
1	A	3/3	X	-	X
2	A	3/3	X	-	X
	B	3/3	-	X	-

<b>Method/Comments:</b>	Venipuncture of the jugular vein (under isoflurane anesthesia). The tail vein may be used if blood cannot be obtained via the jugular vein.
<b>Target Volume (mL):</b>	0.3
<b>Anticoagulant:</b>	K <sub>2</sub> EDTA
<b>Special requirements:</b>	Tubes will be chilled after blood collection.
<b>Processing:</b>	Plasma

X = Sample to be collected; M = Male; F = Female; - = Not applicable

<sup>a</sup> Sample to be collected before the second daily dose.

**S3 Table. Cytokine sample collection for the rat toxicity study**

Group No.	No. of Animals (M/F)	(Time Post the first daily dose) on Day 28		
		0 <sup>a</sup> hr	4 hr	24 hr
3	3/3	X	X	X
4	3/3	X	X	X

<b>Method/Comments:</b>	Venipuncture of the jugular vein (under isoflurane anesthesia). The tail vein may be used if blood cannot be obtained via the jugular vein.
<b>Target Volume (mL):</b>	0.3
<b>Anticoagulant:</b>	K <sub>2</sub> EDTA
<b>Special requirements:</b>	Tubes will be chilled on wet ice after blood collection.
<b>Processing:</b>	Plasma

X = Sample to be collected; M = Male; F = Female; - = Not applicable

<sup>a</sup> Sample to be collected before dosing.

**S4 Table. Human tissue cross-reactivity; list of tissues examined.**

Binding of anti-SARS-CoV-2 RBD IgY was determined using the following normal human tissue from 3 separate donors.

Adrenal	Liver	Spinal Cord
Bladder (urinary)	Lung	Spleen
Blood Cells <sup>a</sup>	Lymph Node	Striated Muscle (skeletal)
Blood Vessels (endothelium) <sup>b</sup>	Ovary	Testis
Bone Marrow	Nasal Mucosa	Thymus
Brain - cerebellum	Pancreas	Thyroid
Brain - cerebral cortex	Parathyroid	Tongue
Breast (mammary gland)	Peripheral Nerve	Tonsil
Eye	Pituitary	Trachea
Fallopian Tube (oviduct)	Placenta	Ureter
Gastrointestinal (GI) Tract <sup>c</sup>	Prostate	Uterus - cervix
Heart	Salivary Gland	Uterus- endometrium
Kidney (glomerulus, tubule)	Skin	

<sup>a</sup> Evaluated from peripheral blood smears.

<sup>b</sup> Evaluated from all tissues where present.

<sup>c</sup> Included esophagus, large intestine/colon, small intestine, and stomach (including underlying smooth muscle).